

DNA methylation analysis in patients with neurodevelopmental disorders improves variant interpretation and reveals complexity

Slavica Trajkova,⁸ Jennifer Kerkhof,² Matteo Rossi Sebastiano,^{4,5} Lisa Pavinato,¹ Enza Ferrero,¹ Chiara Giovenino,¹ Diana Carli,¹ Eleonora Di Gregorio,⁶ Roberta Marinoni,⁶ Giorgia Mandrile,⁷ Flavia Palermo,⁷ Silvia Carestiatto,⁸ Simona Cardaropoli,⁹ Verdiana Pullano,⁸ Antonina Rinninella,^{6,10} Elisa Giorgio,^{11,12} Tommaso Pippucci,¹³ Paola Dimartino,¹¹ Jessica Rzasz,² Kathleen Rooney,^{2,3} Haley McConkey,^{2,3} Aleksandar Petlichkovski,¹⁴ Barbara Pasini,^{1,6} Elena Sukarova-Angelovska,¹⁵ Christopher M. Campbell,¹⁶ Kay Metcalfe,¹⁶ Sarah Jenkinson,¹⁶ Siddharth Banka,^{16,17} Alessandro Mussa,^{9,18} Giovanni Battista Ferrero,¹⁹ Bekim Sadikovic,^{2,3,20} and Alfredo Brusco^{6,8,20,21,*}

Summary

Analysis of genomic DNA methylation by generating epigenetic signature profiles (episignatures) is increasingly being implemented in genetic diagnosis. Here we report our experience using episignature analysis to resolve both uncomplicated and complex cases of neurodevelopmental disorders (NDDs). We analyzed 97 NDDs divided into (1) a validation cohort of 59 patients with likely pathogenic/pathogenic variants characterized by a known episignature and (2) a test cohort of 38 patients harboring variants of unknown significance or unidentified variants. The expected episignature was obtained in most cases with likely pathogenic/pathogenic variants (53/59 [90%]), a revealing exception being the overlapping profile of two *SMARCB1* pathogenic variants with *ARID1A/B:c.6200*, confirmed by the overlapping clinical features. In the test cohort, five cases showed the expected episignature, including (1) novel pathogenic variants in *ARID1B* and *BRWD3*; (2) a deletion in *ATRX* causing MRXFH1 X-linked mental retardation; and (3) confirmed the clinical diagnosis of Cornelia de Lange (CdL) syndrome in mutation-negative CdL patients. Episignatures analysis of the in BAF complex components revealed novel functional protein interactions and common episignatures affecting homologous residues in highly conserved paralogous proteins (SMARCA2 M856V and SMARCA4 M866V). Finally, we also found sex-dependent episignatures in X-linked disorders. Implementation of episignature profiling is still in its early days, but with increasing utilization comes increasing awareness of the capacity of this methodology to help resolve the complex challenges of genetic diagnoses.

Introduction

Neurodevelopmental disorders (NDDs) are a group of heterogeneous childhood conditions that include developmental delay, intellectual disability, language delay, and epilepsy. These disorders are characterized by an underlying heritable component affecting different genes whose products are often part of complex pathways required for different stages of embryonic neurodevelopment. Alongside their genetic heterogeneity, NDDs are characterized by broad phenotypic diversity in their clinical presenta-

tion, which is the major confounding factor when trying to establish genotype-phenotype correlations.¹

Both technical advances and cost reductions have allowed chromosomal microarrays (CMAs) and exome sequencing (ES) to emerge as the tier 1 genomic applications for NDD diagnostics. These methods are now widely used and recommended in clinical practice.^{2–4} Although often successful in detecting underlying genetic causes, a large proportion of cases remain unsolved using these methods. Several factors that can negatively affect the detection rate of causative variants include technical

¹Department of Medical Sciences, University of Turin, 10126 Turin, Italy; ²Verspeeten Clinical Genome Centre, London Health Sciences Centre, London, ON N6A5W9, Canada; ³Department of Pathology and Laboratory Medicine, Western University, London, ON N6A3K7, Canada; ⁴Molecular Biotechnology Center “Guido Tarone” University of Turin, 10126 Turin, Italy; ⁵Department of Molecular Biotechnology and Health Sciences, University of Turin, CASSMedChem, 10126 Turin, Italy; ⁶Medical Genetics Unit, Città della Salute e della Scienza University Hospital, 10126 Turin, Italy; ⁷Medical Genetics Unit and Thalassemia Center, San Luigi University Hospital, Orbassano, TO 10049, Italy; ⁸Department of Neurosciences Rita Levi-Montalcini, University of Turin, Turin 10126, Italy; ⁹Department of Public Health and Pediatric Sciences, University of Turin, 10126 Turin, Italy; ¹⁰Department of Biomedical and Biotechnological Sciences, Medical Genetics, University of Catania, 94124 Catania, Italy; ¹¹Department of Molecular Medicine, University of Pavia, 27100 Pavia, Italy; ¹²Neurogenetics Research Center, IRCCS Mondino Foundation, 27100 Pavia, Italy; ¹³IRCCS Azienda Ospedaliero-Universitaria di Bologna, 40138 Bologna, Italy; ¹⁴Department of Immunology and Human Genetics, Faculty of Medicine, University “Sv. Kiril I Metodij”, Skopje 1000, Republic of Macedonia; ¹⁵Department of Endocrinology and Genetics, Faculty of Medicine, University “Sv. Kiril I Metodij”, Skopje 1000, Republic of Macedonia; ¹⁶Manchester Centre for Genomic Medicine, St. Mary’s Hospital, Manchester University NHS Foundation Trust, Health Innovation Manchester, Manchester M13 9WL, UK; ¹⁷Division of Evolution, Infection & Genomics, Faculty of Biology, Medicine and Health, The University of Manchester, Manchester M13 9WL, UK; ¹⁸Pediatric Clinical Genetics Unit, Regina Margherita Childrens’ Hospital, 10126 Turin, Italy; ¹⁹Department of Clinical and Biological Sciences, University of Turin, 10043 Turin, Italy

²⁰These authors contributed equally

²¹Lead contact

*Correspondence: alfredo.brusco@unito.it

<https://doi.org/10.1016/j.xhgg.2024.100309>.

© 2024 The Authors. This is an open access article under the CC BY license (<http://creativecommons.org/licenses/by/4.0/>).



limitations, such as focusing solely on analyzing coding sequences or potentially overlooking insertions or deletions or small exon deletions. A further explanation resides in our inability to establish a causal relationship between a change in DNA sequence and the clinical presentation of the patient. Such DNA changes are classified as variants of uncertain clinical significance (VUS). Among the reasons for classifying a variant as a VUS are (1) the patient's phenotype does not entirely correspond with the known phenotypes associated with the gene in question; (2) family segregation analyses are missing; or (3) functional assays that prove the causative role of a variant are unavailable. In these patients, a paradigm change has led to the development of new diagnostic tools that are no longer based on modifications in the genome, but based on studying changes in the methylation status of the genome, or epigenome.

Changes in DNA or histone methylation have been identified in a variety of human diseases and, more relevantly for us, in patients with NDDs.^{5,6} Indeed, numerous NDDs have been categorized as chromatinopathies, caused by variants in genes encoding proteins that are part of the epigenetic methylating machinery. These proteins function variously as writers, erasers, readers, or remodelers of chemical chromatin marks.⁷ Malfunction of these proteins is expected to have various downstream epigenetic consequences. These consequences include subtle changes in DNA methylation (DNAm) across the genome; these changes occur early in embryonic development in numerous tissues, including cells of peripheral blood.^{6,8}

An expanding number of chromatinopathies have been shown to have unique genomic DNAm patterns named epigenetic signatures, or episignatures.⁹ As highly sensitive and specific biomarkers, these episignatures represent a quick and specific assay for a particular gene involved in NDD pathogenesis, and can be applied to classify variants of dubious clinical significance. Currently, more than 65 rare disorders exhibit a distinctive genome-wide DNAm profile when analyzed with the EpiSign v.3 clinical methylation assay.¹⁰ As the data from EpiSign assays accumulate, novel features of episignatures are starting to emerge. For example, (1) we now know that variants in genes which do not encode for chromatin-related genes can also present distinctive episignatures^{11,12}; (2) the same episignature may be exhibited by variants in genes which encode for multi-protein complexes, as is the case of the so-called BAFopathies, which affect the components of BAF protein complex¹³; (3) the same gene may exhibit different episignatures, depending on the protein domain where the variant is located, as in the complex NDD Helsmoortel-Van der Aa syndrome (OMIM: 615873)¹⁴; and (4) even single amino acid changes can have a distinct episignature (SMARCA4 M886V).¹⁰ Finally, copy number variants (CNVs) associated with a genomic disorder can also show distinct DNAm patterns.^{15,16}

In this report, we describe our experience of using the EpiSign assay and episignature analysis with a study cohort of 97 patients with NDDs.

Material and methods

Study cohort

Our study group comprised 97 unrelated patients with NDDs selected from a large project focused on genetic screening of NDD cases (NeuroWES). Patients were evaluated by an experienced pediatrician and/or clinical geneticist who provided the phenotype and, when needed, reverse phenotyping. The patients were divided into three categories (see [Tables 1](#) and [S1](#)): (1a) validation cohort #1a, which consisted of 34 NDD cases with pathogenic or likely pathogenic single nucleotide variants (SNVs) in a gene with known disease-specific methylation patterns or episignatures that are listed in the EpiSign v.3 classifier; (1b) validation cohort #1b, which consisted of 25 NDD cases with pathogenic or likely pathogenic CNVs that are also listed in the EpiSign v.3 classifier; (2) an uncertain cohort composed of 18 NDD cases with an SNV/CNV VUS or with a strong clinical suspicion but no specific variant identified, and (3) 20 unresolved NDD cases defined by females or mothers of unresolved male cases that showed skewed X chromosome inactivation (XCI) of more than 80% (Supplemental Materials and methods).¹⁷

All SNVs were confirmed by Sanger sequencing; both SNVs and CNVs were classified according to the American College of Medical Genetics and Genomics (ACMG)/Association for Molecular Pathology (AMP) guidelines.^{18–20} Genomic sequencing for case 150163 is reported in Supplemental Materials and methods.

Sample and microarray processing

DNAm array data were performed using MethylationEPIC Bead-Chip array (EPIC array) at the Verspeeten Clinical Genome Center, London Health Sciences Center in London, Canada, following the manufacturer's protocols and analyzed at the same center, as previously described.^{10,21,22} Methylation data for each sample were compared with all 57 DNAm profiles (associated with 65 genetic syndromes) included in the EpiSign v.3 classifier.

DNAm analysis by EpiSign

The DNAm data for each sample was compared to the EpiSign Knowledge Databases (EKDs) using the support vector machine (SVM)-based classification algorithm as previously described.^{10,21,22} The EKD includes thousands of clinical peripheral blood DNAm profiles from disorder-specific reference and normal controls (general population samples with various age and racial backgrounds). The SVM decision values were converted to methylation variant pathogenicity (MVP) scores ranging from 0 to 1, using the Platt scaling method. MVP scores indicate the prediction confidence for the specific episignature. Scores of greater than 0.01 undergo a secondary review using hierarchical and multidimensional scaling (MDS) clustering plots associated with the episignature. The final EpiSign result is a combination of the three assessed parameters: MVP scores, hierarchical plots, and MDS plots. The result is reported with a confidence level relative to the reference episignature cohorts, where high confidence indicates agreement among all three parameters and moderate confidence indicates disagreement in at least one of the three parameters.

Three-dimensional protein modeling

The BAF complex model was constructed by selecting suitable experimental structures to be used as scaffold and by superposing the corresponding human proteins in their full-length version as

Table 1. Cases tested using EpiSign v.3 classifier

Sample ID	Sex	Gene	Variant	ACMG/ AMP	Phenotype/ diagnosis ^a	Epi V4 result	Notes
1a) Validation cohort: SNVs in genes with known epesignatures (34 cases)							
1	NWM-030D	F	<i>ADNP</i>	NM_001282531.3: c.539_542del p.(Val180fs)	P	HVDAS	HVDAS_T <i>ADNP</i> C-term sign.
2	GM223306	F	<i>ADNP</i>	NM_001282531.3: c.2454C>G p.(Tyr818Ter)	P	HVDAS	HVDAS_T <i>ADNP</i> C-term sign.
3	121623	M	<i>ANKRD11</i>	NM_013275.6: c.439C>T p.(Gln147Ter)	P	KBGS	KBGS
4	BA2012002	F	<i>ANKRD11</i>	NM_013275.6: c.211_226+1del p.?	P	KBGS	KBGS
5	NWM-218D	M	<i>ANKRD11</i>	NM_013275.6: c.1903_1907del p.(Lys635fs)	P	KBGS	KBGS
6	NMW-035D	M	<i>ARID1A</i>	NM_006015.6: c.6232G>A p.(Glu2078Lys)	LP	CSS2	CSS_c.6200 subregion epesignature
7	160759	F	<i>ARID1B</i>	NM_001374828.1: c.5825G>A p.(Trp1942Ter)	LP	CSS1	BAFopathy broad BAFopathy epis.
8	142220	M	<i>CHD7</i>	NM_017780: c.3082A>G p.(Ile1028Val)	LP	CHARGE	CHARGE
9	FS0208013	M	<i>CHD7</i>	NM_017780: c.6194G>A p.(Arg2065His)	LP	CHARGE	CHARGE
10	110562	M	<i>CHD8</i>	NM_001170629.2: c.2025-1G>C p.?	LP	IDDAM	IDDAM
11	110212	M	<i>CREBBP</i>	NM_004380.3:c.3779 + 1G>A p.?	P	RSTS1	RSTS broad RSTS epis.
12	141444	M	<i>EHMT1</i>	NM_024757.5: c.3331T>A p.(Cys1111Ser)	P	KLEFS1	KLEFS broad KLEFS epis.
13	131361	M	<i>EHMT1</i>	NM_024757.5: c.3001del p.(Asp1001fs)	P	KLEFS1	KLEFS broad KLEFS epis.
14	GM181933	M	<i>EHMT1</i>	NM_024757.5: c.508del p.(Gln170fs)	P	KLEFS1	KLEFS broad KLEFS epis.
15	GM184039	F	<i>EP300</i>	NM_001429.4: c.3671 + 5G>C p.?	LP	RSTS2	RSTS1 discordant
16	NWM-019D	M	<i>EZH2</i>	NM_004456.5: c.2015T>G p.(Phe672Cys)	LP	WVS	PRC2
17	NWM-088D	F	<i>HIST1H1E</i>	NM_005321.3: c.458_460del p.(Lys152fs)	P	RMNS	RMNS
18	GM201880	F	<i>KAT6A</i>	NM_006766.5: c.2927del p.(Gly976Valfs)	P	ARTHS	ARTHS
19.1	121116	M	<i>KDM5C</i>	NM_004187.5: c.1204G>A p.(Asp402Asn)	LP	MRXSCJ	MRXSCJ discordant
19.2	121886	F	<i>KDM5C</i>	NM_004187.5: c.1204G>A p.(Asp402Asn)	LP	MRXSCJ	
19.3	121888	F	<i>KDM5C</i>	NM_004187.5: c.1204G>A p.(Asp402Asn)	LP	MRXSCJ	negative discordant
20	NWM-192D	F	<i>KMT2A</i>	NM_001197104.2: c.4777del p.(Arg1593fs)	P	WDSTS	WDSTS
21	GM194228	M	<i>KMT2D</i>	NM_003482.4: c.4395dup p.(Lys1466fs)	P	KABUK1	Kabuki
22	NWM-031D	F	<i>KMT2D</i>	NM_003482.4: c.13795_13802del p.(Ala4599fs)	P	KABUK1	Kabuki
23	NWM-024D	F	<i>PHF6</i>	NM_001015877.2: c.890G>T p.(Cys297Phe)	LP	BFLS	negative discordant
24.1	NWM-163D1	M	<i>PQBP1</i>	NM_001032383.2: c.457_459del p.(Arg153fs)	P	RENS1	RENS1
24.2	NWM-163D2	M	<i>PQBP1</i>	NM_001032383.2: c.457_459del p.(Arg153fs)	P	RENS1	RENS1

(Continued on next page)

Table 1. Continued

	Sample ID	Sex	Gene	Variant	ACMG/ AMP	Phenotype/ diagnosis ^a	Epi V4 result	Notes
25	GM182051	M	<i>PQBP1</i>	NM_001032383.2: c.233C>A p.(Pro78Gln)	LP	RENS1	RENS1	
26	GM173348	F	<i>SETD1B</i>	NM_001353345.2: c.598_600del p.(Gln200fs)	P	IDDSELD	IDDSELD	
27	GM223349	M	<i>SETD5</i>	NM_001080517.3: c.868_872del p.(Arg290fs)	P	MRD23	MRD23	
28	GM223350	F	<i>SETD5</i>	NM_001080517.3: c.3848_3849insC p.(Ser1286fs)	P	MRD23	MRD23	
29	GM190941	M	<i>SMARCA4</i>	NM_003072.5: c.3068A>G p.(Glu1023Gly)	LP	CSS4	negative	discordant
30	GM223379	F	<i>SMARCA4</i>	NM_003072.5: c.1646G>T p.(Arg549Leu)	LP	CSS4	negative	discordant
31	GM223380	F	<i>SMARCB1</i>	NM_003073.5: c.110G>A p.(Arg37His)	LP	CSS3	CSS_c.6200	discordant
32	GM183514	F	<i>SMC1A</i>	NM_006306.4: c.1276_1282del p.(Arg426fs)	LP	CDLS2	CDLS	broad CDLS epis.
33	130091	M	<i>SOX11</i>	NM_006306.4: c.159G>T p.(Met53Ile)	P	CSS9	CSS9	
34	131749	M	<i>SRCAP</i>	NM_006662.3: c.7937_7938del p.(Val2646fs)	P	FLHS	FLHS	
Ib) Validation cohort: CNVs with known EpiSignatures (25 cases)								
1	NWM-020D	F	<i>SETD5</i>	3p25.3(9091710–12334937)x1	P	MRD23	MRD23	
2	162391	M	<i>SETD5</i>	3p26.3(52266–10683525)x1	P	MRD23	MRD23	
3	GM190395	F	<i>4p16.13del</i>	4p16.13(71660–6479683)x1	P	WHS	WHS	
4	GM200157	F	<i>4p16.13del</i>	4p16.13(71660–13395123)x1	P	WHS	WHS	
5	T223	M	<i>5q35del</i>	5q35(176463495–177956831)x1	P	SOTOS	Sotos	
6	S288	M	<i>5q35dup</i>	5q35(176412680–177477797)x3	P	HMA	HMA	
7	GM201583	F	<i>7q11.23del</i>	7q11.23(73312582–74924037)x1	P	WBS	WBS	
8	GM192375	M	<i>7q11.23del</i>	7q11.23(73312582–74725057)x1	P	WBS	WBS	
9	GM193789	F	<i>7q11.23dup</i>	7q11.23(73312582–74725057)x3	P	WBS dup	WBS dup	
10	111884	F	<i>EHMT1</i>	9q34.3(136428708–138059695)x1	P	KLEFS1	KLEFS	broad KLEFS epis.
11	131568	F	<i>EHMT1</i>	9q34.3(137447506–137984409)x1	P	KLEFS1	KLEFS	broad KLEFS epis.
12	161978	M	<i>EHMT1</i>	9q34.3(135866376–138114463)x1	P	KLEFS1	KLEFS	broad KLEFS epis.
13	GM181473	F	<i>EHMT1</i>	9q34.3(137666340–138059695)x1	P	KLEFS1	KLEFS	broad KLEFS epis.
14	N821	F	<i>CREBBP</i>	16p13.3(3461539–3805666)x1	P	RSTS1?	RSTS1	
15	112066	M	<i>22q11.21del</i>	22q11.21(18932429–21086225)x1	P	VCFS/DGS	VCFS/DGS	22q11.21DS LCR A-D
16	112408	M	<i>22q11.21del</i>	22q11.21(18932429–21086225)x1	P	VCFS/DGS	VCFS/DGS	22q11.21DS LCR A-D
17	141583	M	<i>22q11.21del</i>	22q11.21(18932429–21086225)x1	P	VCFS/DGS	VCFS/DGS	22q11.21DS LCR A-D

(Continued on next page)

Table 1. Continued

	Sample ID	Sex	Gene	Variant	ACMG/ AMP	Phenotype/ diagnosis ^a	Epi V4 result	Notes
18	160892	M	<i>22q11.21del</i>	22q11.21(18932429–21086225)x1	P	VCFS/DGS	VCFS/DGS	22q11.21DS LCR A-D
19	161876	F	<i>22q11.21del</i>	22q11.21(18932429–21086225)x1	P	VCFS/DGS	VCFS/DGS	22q11.21DS LCR A-D
20	GM192617	F	<i>22q11.21del</i>	22q11.21(18932429–21086225)x1	P	VCFS/DGS	VCFS/DGS	22q11.21DS LCR A-D
21	150284	M	<i>22q11.21del</i>	22q11.21(18932429–20324240)x1	P	VCFS/DGS	VCFS/DGS	22q11.21DS LCR A-B
22	162620	M	<i>22q11.21del</i>	22q11.21(18932429–20324240)x1	P	VCFS/DGS	VCFS/DGS	22q11.21DS LCR A-B
23	142071	F	<i>17q21.3del</i>	17q21.3(45640337–46082496)x1	P	KDVS	KDVS	
24	152118	F	<i>17q21.3del</i>	17q21.3(45640337–46082496)x1	P	KDVS	KDVS	
25	GM181681	F	<i>17q21.3del</i>	17q21.3(45640337–46267672)x1	P	KDVS	KDVS	
2) Confirmation of pathogenicity in cases with VUS (SNV/CNV) or clinical suspicion without any variant found (18)								
1	160708	M	<i>ARID1B</i>	NM_001374828.1: c.2480C>T p.(Ala827Val)	VUS	CSS1	BAFopathy	broad BAFopathy epis.
2	150163	M	<i>ARID1B</i>	NM_001374828.1: c.3589G>A p.(Asp1197Asn)	VUS	CSS1	CdLS	new diagnosis suggested
3	NWM-116D	M	<i>BRWD3</i>	NM_153252.5: c.1233-7_1233-3del p.?	VUS	MRX93	MRX93	VUS -> LP
4	GM173400	F	<i>SMARCA2</i>	NM_003070.5: c.2566A>G p.(Met856Val)	VUS	NCBRS	BIS	discordant
5	GM203135	F	<i>KMT2A</i>	NM_001197104.2: c.5959G>A p.(Glu1987Lys)	VUS	NDD	negative	VUS -> LB
6.1	140556	M	<i>SMARCA2</i>	NM_003070.5: c.2296C>G p.(Leu766Val)	VUS	NCBRS	negative	VUS -> LB
6.2	140558	M	<i>SMARCA2</i>	NM_003070.5: c.2296C>G p.(Leu766Val)	VUS	NCBRS	negative	VUS -> LB
7	NWM-236D	F	<i>NIPBL</i>	No variant identified	–	CdLS	CdLS	new diagnosis suggested
8	S890	M	<i>22q11.21del</i>	22q11.21(20379137–21151128)x1	VUS	VCFS/DGS	VCFS/DGS	22q11.21DS LCR B-D
9	GM203534	F	<i>22q11.21del</i>	22q11.21(20400132–21086225)x1	VUS	VCFS/DGS	negative	22q11.21DS LCR B-D
10	140901	F	<i>22q11.21del</i>	22q11.21(20400132–21086225)x1	VUS	VCFS/DGS	Negative	22q11.21DS LCR B-D
11	R641	M	<i>22q11.21del</i>	22q11.21(21444416–22574173)x1	VUS	VCFS/DGS	negative	22q11.21DS LCR B-D
12	141494	F	<i>22q11.21del</i>	22q11.21(21444416–22574173)x1	VUS	VCFS/DGS	negative	22q11.21DS LCR B-D
13	S257	F	<i>22q11.21del</i>	22q11.21(20721287–21025669)x1	VUS	VCFS/DGS	negative	
14	131777	M	<i>22q11.21del</i>	22q11.22(21968733–22215491)x1	VUS	VCFS/DGS	negative	
15	GM194370	M	<i>22q11.21del</i>	22q11.22(21968733–22215491)x1	VUS	VCFS/DGS	negative	
16	GM193223	M	<i>22q11.21del</i>	22q11.22(21968733–22215491)x1	VUS	VCFS/DGS	negative	
17	GM191544	M	<i>22q11.21del</i>	22q11.22(22655814–23285204)x1	VUS	VCFS/DGS	negative	
18	GM193550	M	<i>22q11.21del</i>	22q11.22(22655814–23285204)x1	VUS	VCFS/DGS	negative	

(Continued on next page)

Table 1. Continued

	Sample ID	Sex	Gene	Variant	ACMG/ AMP	Phenotype/ diagnosis ^a	Epi V4 result	Notes
3) Cases with skewed XCI (20)								
1	NWM-021D	F		No variant identified; sk.-XCI (97%)		NDD	MRD23/KBGS	new diagnosis suggested
2	141078	M		No variant identified; sk.-XCI (92%)		NDD		
3	162199	M		No variant identified; sk.-XCI (91%)		NDD		
4	150692	M		No variant identified; sk.-XCI (95%)		NDD		
5	140041	M		No variant identified; sk.-XCI (90%)		NDD		
6	160035	M		No variant identified; sk.-XCI (88%)		NDD		
7	152994	F		No variant identified; sk.-XCI (93%)		NDD		
8	141345	F		No variant identified; sk.-XCI (94%)		NDD		
9	GM210581	F		No variant identified; sk.-XCI (100%)		NDD		
10	150689	F		No variant identified; sk.-XCI (55%) ^b		NDD		
11	GM170809	F		No variant identified; sk.-XCI (84%)		NDD		
12	29D	F		No variant identified; sk.-XCI (97%)		NDD		
13	6D	F		No variant identified; sk.-XCI (95%)		NDD		
14	173D	F		No variant identified; sk.-XCI (93%)		NDD		
15	164D	M		No variant identified; sk.-XCI (96%)		NDD		
16	FM0-711016_92	M		No variant identified; sk.-XCI (100%)		NDD		
17	90D	M		No variant identified; sk.-XCI (94%)		NDD		
18	43D	M		No variant identified; sk.-XCI (91%)		NDD		
19	22D	M		No variant identified; sk.-XCI (91%)		NDD		
20	111092	M	<i>ATRX</i>	<i>ATRX</i> exon 3–4 deletion; sk.-XCI (100%)	P	MRXFH1	MRXFH1	case solved by episign.

ARTHS, Arboleda-Tham syndrome (OMIM: 616268); CDLS1, Cornelia de Lange syndrome-1 (OMIM:122470); CDLS2, Cornelia de Lange syndrome-2 (OMIM: 300590); CSS1, Coffin-Siris syndrome-1 (OMIM: 135900); CSS2, Coffin-Siris syndrome-2 (OMIM: 614607); CSS3, Coffin-Siris syndrome-3 (OMIM: 614608); CSS4, Coffin-Siris syndrome-4 (OMIM: 614609); CSS9, Coffin-Siris syndrome-9 (OMIM: 615866); HMA, Hunter-McAlpine (OMIM 601379); HVDAS, Helsmoortel-Van der Aa syndrome (OMIM: 615873); IDDAM, intellectual developmental disorder with autism and macrocephaly (OMIM: 615032); IDDSILD, intellectual developmental disorder with seizures and language delay (OMIM: 619000); KABUK1, Kabuki syndrome-1 (OMIM: 147920); KBGS, KBG syndrome (OMIM: 148050); KDVS, Koolen-De Vries syndrome (OMIM: 610443); KLEFS1, Kleefstra syndrome-1 (OMIM: 610253); MRD23, autosomal dominant intellectual developmental disorder-23 (OMIM: 615761); MRXSJ, Claes-Jensen type of X-linked syndromic intellectual developmental disorder (OMIM: 300534); MRX93-Mental retardation X-linked 93 CHARGE (OMIM: 214800); MRXFH1, X-linked intellectual disability-hypotonic facies syndrome-1 (OMIM: 309580); NDD, neurodevelopmental disorder; RENS1, Renpenning syndrome (OMIM: 309500); RMNS, Rahman syndrome (OMIM: 617537); sk-XCI, skewed XCI >80%; SOTOS, Sotos syndrome (OMIM: 117550); WBS, Williams-Beuren syndrome (OMIM: 194050); WBS dup, duplication of genes lying within the critical region for Williams-Beuren syndrome (OMIM: 609757); WDSTS, Wiedemann-Steiner syndrome (OMIM: 605130); WHS, Wolf-Hirschhorn syndrome (OMIM: 194190); WVS, Weaver syndrome (OMIM: 277590); X-linked intellectual developmental disorder-93 (OMIM: 300659). Numbering of patients: 19.1, 19.2, 19.3, 24.1, 24.2, 6.1, and 6.2 refers to siblings carrying the same genetic variant.

^aThe phenotype indicated is the clinical diagnosis of the reported case. A question mark indicates a suspected diagnosis.

^bThe proband's mother (case 150691) was 95% skewed.

found in the Alpha Fold Database. Specifically, the full BAF complex was constructed based on the work of He and co-workers.²³ The structure used as template was resolved with cryo electron microscopy; the PDB code is 6LTJ, the resolution is 3.70 Å. The AlphaFold structures for the human full-length SMARCB1 and ARID1A/B were superposed (UniProt accession Nos. Q12824, O14497, and Q8NFD5). The BAF base module originated from the PDB structure 6LTH (cryo electron microscopy, human, resolution 3.00 Å).

All protein structure manipulations were performed with the Molecular Operating Environment (version 2022), from ChemComp (www.chemcomp.com) by first employing the structure preparation pipeline with standard settings. Then, PDB templates and AlphaFold models were imported in the same session and superposed with the check and realign procedure. Finally, hydrogens were added and partial charges assigned according to the parameters of the AMBER 10:EHT forcefield.²⁴ Then the overall structure was inspected for clashes after removing the original chains in the PDB template. Clashes were avoided with multiple local minimization cycles and a final global minimization was performed, obtaining models hosting full-length SMARCB1 and ARID1A/B chains. The procedure was obtained for the wild-type complex or by introducing the selected mutations with the MOE protein builder tool (www.chemcomp.com). Before global minimization, sidechain optimization for the mutant residue was performed. The interaction energy between SMARCB1 and ARID1A/B in the complex was estimated through the MOE energy tool and considered the sum of all terms. The same procedure for chain superposition was obtained when comparing the structures of SMARCA2 and SMARCA4 (UniProt references P51531 and P51532, respectively). The sequence alignment was based on the BLOSUM62 matrix and the structural component considered alpha carbons. All other settings of the superposition were default.

For the determination of newly formed interactions, standard MOE cutoffs were considered and the choice of relevant atoms to display relative distance was made upon visual inspection.

Ethics approval and consent to participate

All individuals and families from the different institutions agreed to participate in this study and signed appropriate consent forms according to the Declaration of Helsinki [Ethics Committee of University of Turin (n. 0060884) and University of Skopje (n. 03–6116/7)]. Consent for publication has been obtained from individuals or their parent or legal guardian in case of children, whose clinical details or images are reported.

Results

Characteristics of the cohorts used for episinature analysis

This study involving episinature analysis is based on a cohort of 97 unrelated patients with NDDs (Table 1), divided into the following groups: (1a) the SNV validation cohort, which analyzed DNA samples from 34 cases with likely pathogenic or pathogenic SNVs in disease-associated genes with an established diagnostic EpiSign methylation profile; (1b) the CNV validation cohort, which analyzed DNA samples from 25 cases with likely pathogenic or pathogenic CNVs involving 26 different genes/CNVs with an established diagnostic EpiSign methylation profile¹⁰; (2)

the VUS/undetected variant cohort, which consisted of 18 samples from patients with either a VUS (SNV or CNV) or with a clinically suspected NDD but no variant detected by preceding genome analyses; (3) the skewed XCI cohort, which consisted of 20 samples with a clinical diagnosis of NDD, without a causative X-linked variant identified by exome analysis.

EpiSign analysis of the SNV and CNV control cohorts

The combined SNV validation cohort (34 samples) and the CNV validation cohort (25 samples) represented our 59 control samples where the EpiSign profile expected of the SNV/CNV is known *a priori*.¹⁰ In fact, in 53 of the 59 specimens analyzed (28/34 SNVs; 25/25 CNVs), the methylation pattern obtained correctly matched the established EpiSign profile, identifying the correct episinatures that were gene/CNV-specific, protein domain-specific (e.g., *ADNP* central nonsense variants in Helsmoortel-Van der Aa syndrome) or protein complex-specific (e.g., pertaining to the BAFopathies, Cornelia De Lange syndrome [CdLS]), or Kabuki syndrome) (Table 1).

Discordant results were obtained in 6 of 34 SNV validation cohort samples. Of these, three did not match the expected episinature (Table 1; samples GM184039, 121116, and GM223380) and three did not match any known episinature (Table 1; samples GM190941, GM223379, and NWM-024D). These samples were further investigated to unravel the causes of the discordance.

Sample GM184039

The patient (female) is heterozygous for a *de novo* likely pathogenic splicing variant (c.3671+5G>C p.?) in *EP300*, the gene where truncating variants are associated with Rubinstein-Taybi syndrome 2 (RSTS2) (OMIM: 613684). However, the observed methylation profile suggested Rubinstein-Taybi syndrome 1 (RSTS1) (OMIM: 180849), which is associated with the *EP300* partner and paralog, *CREBBP*. This result might suggest that this variant has unexpected effects on the function of the CREBBP/EP300 acetyltransferase complex. In addition, global methylation analysis also revealed hypomethylation at the *GNAS* A/B:TSS-DMR locus, suggestive of pseudohypoparathyroidism, type 1B (PHP1B) (OMIM: 603233). These findings led to a clinical re-evaluation of the patient,²⁵ who had slightly increased parathyroid hormone levels and brachydactyly, although other PHP1B-related features (e.g., skeletal, renal, and biochemical abnormalities) were absent. Additional studies are ongoing to confirm the role of the *EP300* variant and the possibility that the distinctive methylation profile may be caused by the overlap of these two conditions.

Sample 121116

The patient (male) has a hemizygous variant c.1204G>A p.(D402N) in *KDM5C*, a histone demethylase-encoding gene associated with Claes-Jensen syndrome (MRXSCJ) (OMIM: 300534), an X-linked recessive disorder.¹⁷ The clinical features suggested a milder form of MRXSCJ and the observed episinature was consistent with that

of a heterozygous female, supporting this interpretation (Figure S1). We further extended methylation profiling to his sister and mother (cases 19.2 and 19.3) (Table 1), who were carriers of the variant, but without a reported phenotype. In women, the methylation profile was not concordant with MRXSCJ cases; however, the sister clustered with carriers and the mother with controls, although slightly shifted toward heterozygous females (Figure S1). The third discordant sample, GM223380, is discussed with the BAFopathy cases.

Samples GM190941 and GM223379

These samples are from two patients that present the clinical features of Coffin-Siris syndrome 4 (CSS4)²⁶ and have likely pathogenic variants in the chromatin remodeler *SMARCA4*, a known CSS4-related gene: c.3068A>G p.(E1023G) in GM190941 and c.1646G>T p.(R549L) in GM223379. We expected the methylation profile to fall within the BAFopathy cluster; instead, both cases revealed an epismature that was intermediate between the BAFopathy profile and the profile of blepharophimosis-impaired intellectual disability syndrome (BIS) (OMIM: 619293), an allelic disorder associated with *SMARCA2*, a paralog of *SMARCA4* (Figure 1A). *SMARCA4* and *SMARCA2* are mutually exclusive catalytic components of the BAF chromatin remodeling complex and their protein sequence alignments show 73% amino acid identity over the whole protein length. Intriguingly, both *SMARCA4* variants substitute paralogue-conserved residues: *SMARCA4* E1023 corresponds with E993 in *SMARCA2*, and *SMARCA4* R549 to *SMARCA2* R525 (Figure S2). Interestingly the facial dysmorphism of case GM223379 resembled more BIS than CSS4 (narrow palpebral fissures, mild blepharophimosis, epicanthal folds, and ptosis).

Sample NWM-024D

The patient (female) has autistic features, global developmental delay, brachy/syndactyly, coarse facial features with strabismus, and was originally described in¹⁷ (Figure 1B). She is heterozygous for a *de novo* variant c.890G>T p.(C297F) in *PHF6*, the causative gene of Borjeson-Forssman-Lehmann syndrome (BFLS) (OMIM: 301900) (Figure S3). The methylation profile was similar to healthy controls and did not match that of BFLS cases (Figure 1C). Since BFLS is an X-linked recessive disorder, affected cases are males, while heterozygous females are usually unaffected or may present a mild clinical phenotype.²⁷ Our proband showed clinical presentation and very similar facial gestalt as the other described female cases carrying a few amino acid distant changes.²⁷ The complete X-inactivation skewing was further supporting an X-linked condition. In this case, we are hypothesizing that a sex-related epismature exists for this gene. Indeed, the BFLS EpiSign profile was obtained from male cases of BFLS; the one other female analyzed so far (GDB1321) (Figure 1C)²² also showed a methylation pattern similar to controls.

Regarding our analysis of CNVs with known epismatures, our study confirmed that 25 of the 25 CNVs were

indeed pathogenic (Table 1). In most cases, these CNVs were associated with contiguous gene syndromes, where a combination of several dosage-sensitive genes causes the disease and likely affects the DNAm pattern. In other cases, the CNV analyzed caused the loss or gain of a single dosage-sensitive gene, revealing a DNAm profile specific for the disease-associated gene in question: e.g., the 5q35 deletion associated with Sotos syndrome involving *NSD1*, the 5q35 duplication associated with Hunter-McAlpine craniosynostosis syndrome (*NSD1*), and the 4p16.13 deletion associated with Wolf-Hirschhorn syndrome (*NSD2*). Among the contiguous gene syndromes, we confirmed two 7q11.23 deletions and one 7q11.23 duplication corresponding with Williams-Beuren syndrome and the reciprocal duplication profiles, respectively. Finally, we confirmed eight cases with the typical 22q11.2DS epismature profile, while the same epismature was excluded in six cases involving variable deletions in the central 22q11.2DS (described below). This confirms previous data suggesting that the 22q11.2DS EpiSign profile is specific for the loss of the 1.5-Mb region known as the Di-George syndrome (DGS)/velocardiofacial syndrome (VCFS) critical region.

EpiSign analysis of the VUS/no variant cohort

In this cohort, we conducted epismature analysis of 18 deeply phenotyped NDD cases with VUS, with the aim of establishing whether or not they were pathogenic. Details of four cases are provided below, where the rest of the cases did not match any of the defined epismature profiles.

Samples 160708 and NWM-116D

Sample 160708 was from a patient with CSS1 with a missense VUS c.2480C>T p.(A827V) in *ARID1B*, the known causative gene of CSS1, which encodes a component of the BAF chromatin remodeling complex. The DNAm profile matched the BAFopathy epismature, allowing us to reclassify the variant as likely pathogenic (Figure 1A).

Sample NWM-116D had a maternally inherited variant predicted to affect the acceptor splice site in exon 14 of *BRWD3* [c.1233-7_1233-3del p.?; predicted change -66%] (Figure S4). Other biological samples were unavailable, making it impossible to confirm aberrant splicing by cDNA analysis, but the patient clinically matched the phenotype of MRX93, intellectual developmental disorder, X-Linked 93 (OMIM: 300659) associated with *BRWD3*. The DNAm pattern confirmed this diagnosis, reclassifying the variant as likely pathogenic.

Samples 150163 and NWM-236D

Sample 150163 was from a patient with a *de novo* *ARID1B* D1197N VUS (Figure 2A). However, the methylation profile was inconsistent with a BAFopathy and instead compatible with the profile in CdLS (Figure 2B). This result suggested that *ARID1B* D1197N was not pathogenic. Indeed, reverse phenotyping of the patient revealed clinical features suggestive of CdLS (Figure 2A), indicating we may have missed the causative variant in one of the

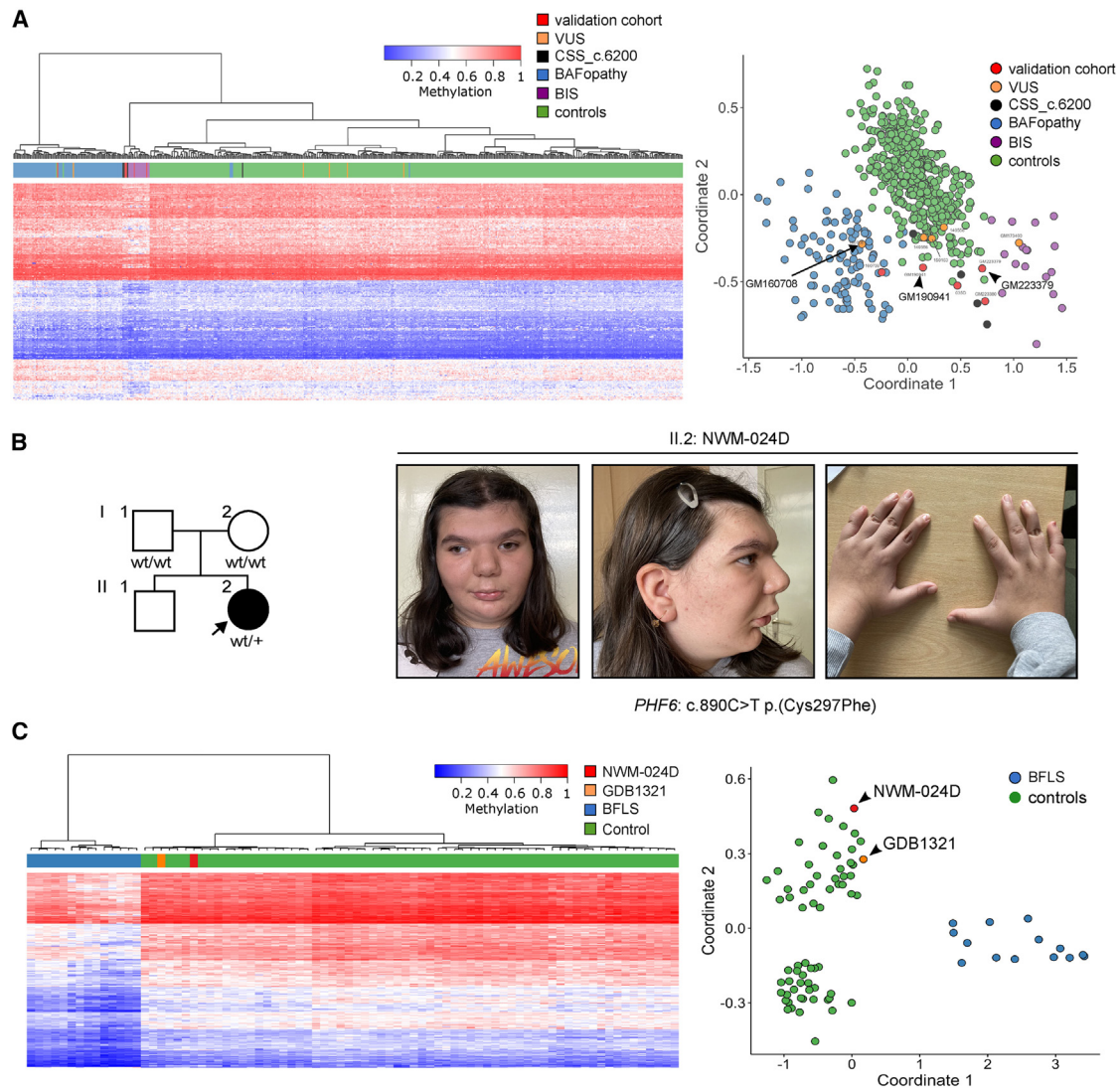


Figure 1. Novel interpretations for discordant epigenatures

(A) Euclidean hierarchical clustering (heatmap) (left) and MDS plot (right) from two subjects with CSS4 that harbored likely pathogenic variants in *SMARCA4*: GM190941 [c.3068A>G p.(E1023G) and GM223379 (c.1646G>T p.(R549L)]. In the MDS, the DNAm methylation profiles of the CSS4 samples do not cluster with the BAFopathy epigenature. The detected epigenature is currently undefined and the two patients uncharacterized. Case GM160708 with *ARID1B*:c.2480C>T p.(A827V) had a BAFopathy EpiSig, supporting the diagnosis of a rare case of CSS1 due to a missense variant in *ARID1B*.

(B) Family tree of patient NWM-024D (II.2), the second child of healthy parents. She had a *de novo* *PHF6*:c.890C>T p.(C297F) variant, strongly suggestive of BFLS. Note the coarse and wide face, low-set ears, bitemporal narrowing, hypertelorism, prominent supraorbital ridges, prominent eyebrows, synophrys, long philtrum, carpe-shaped nose, retrognathia, short neck, and brachydactyly (photo at 12 years of age).

(C) Left shows the DNAm heatmap of two patients with BFLS, NWM-024D, and GDB1321, the latter being the only other female with BFLS so far analyzed, established BFLS cases and healthy controls. Right, the MDS plot shows clustering of NWM-024D and GDB1321²² with controls (green) and not with BFLS cases (blue).

CdLS-associated genes. Further investigation by genome sequencing failed to identify SNVs or structural variants in known CdLS genes (Supplemental materials and methods; Table S2). The CdLS epigenature was also identified in NWM-236D, a second patient whose phenotype suggested CdLS but without detectable anomalies by CMA or ES (Figures 2B, 2D, and 2F), again suggesting a missed pathogenic variant in one of the CdLS genes.

Sample GM173400 with a VUS in *SMARCA2* is discussed below. Samples from patients with VCFS/DGS and CNVs

of unknown significance are examined separately (see below).

EpiSig analysis of the skewed XCI cohort

Our last cohort consisted of probands with NDD with no candidate variants after genome analysis but with a family history of skewed XCI, suggesting a disorder with X-linked inheritance.¹⁷

Among the 20 cases, we found patient NWM-021D had the epigenature specific for MRD23_KBG, intellectual

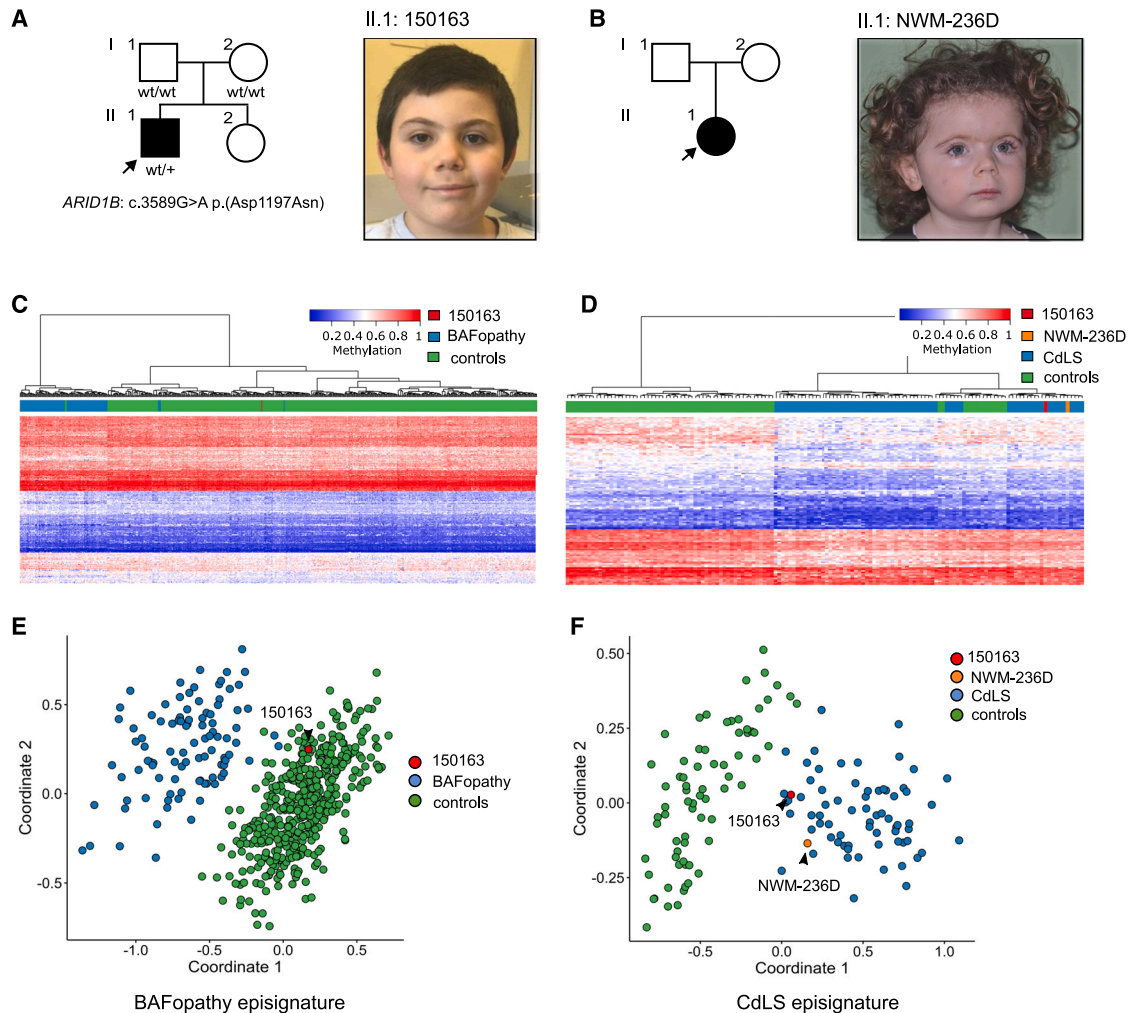


Figure 2. Episignature analysis suggests a diagnosis of CdLS in unsolved cases

(A and B) Cases 150163 and NWM-236D of CdLS with no variants identified in CdLS genes by ES/CMA screening. Case 150163 was initially misleading as he had an *ARID1B* c.3220G>A p.(D1074N) *de novo* missense variant. This variant has now been reported in three cases in GnomAD (v.2.1.1), further supporting its likely benign role.

(C and D) Heatmaps for cases 150163 (C, left) and NWM-236D (D, right).

(E and F) MDS plots for the two patients showed that 150163 did not show a BAFopathy episignature (E, left MDS), whereas both cases clustered with the CdLS profile (F, right MDS).

developmental disorder, autosomal dominant 23 syndrome (formally mental retardation, autosomal dominant 23 syndrome) and KBG syndrome (Figure S5, bottom), although CMA/ES analyses failed to identify deleterious variants in either of the associated genes, i.e., *SETD5* and *ANKRD11*. Among the possible explanations, there may be a missed variant in these genes or a yet unknown genes associated with this episignature.¹⁰

Sample 111092

The clinical features of this male patient suggested X-linked intellectual disability, hypotonic facies syndrome 1 (MRXFH1) (OMIM: 309580), but no variants were detected by genome analysis. The patient's mother was also uninformative, however showing completely skewed XCI. The proband's methylation profile was clearly associated with that of *ATRX*, the causative gene of MRXFH1, which encodes a chromatin remodeler (Figure S5, top).

The case was further studied by our group¹⁷ and finally resolved with the identification of a deletion in *ATRX* of exons 3 and 4 (NM_000489.6: c.134-4884_242+41del p.?).

Expanding BAFopathy complex episignatures

Genes involved in chromatin remodeling/DNA methylation are among the most frequently mutated in NDDs,²⁸ and episignature analysis of the BAFopathies is rapidly evolving into an opportunity to dissect the function of individual BAF complex proteins at the protein domain, sub-domain down to the single amino acid level. Among the most prominent and most studied BAFopathies are the clinically overlapping syndromes CSS and Nicolaides-Baraitser (NCBRS) (MIM: 601358), caused by variants in BAF complex proteins: *ARID1B* in CSS1, *SMARCB1* in CSS2, and *SMARCA4* in CSS4; and *SMARCA2* in NCBRS. Both syndromes are associated with a broad DNAm episignature,

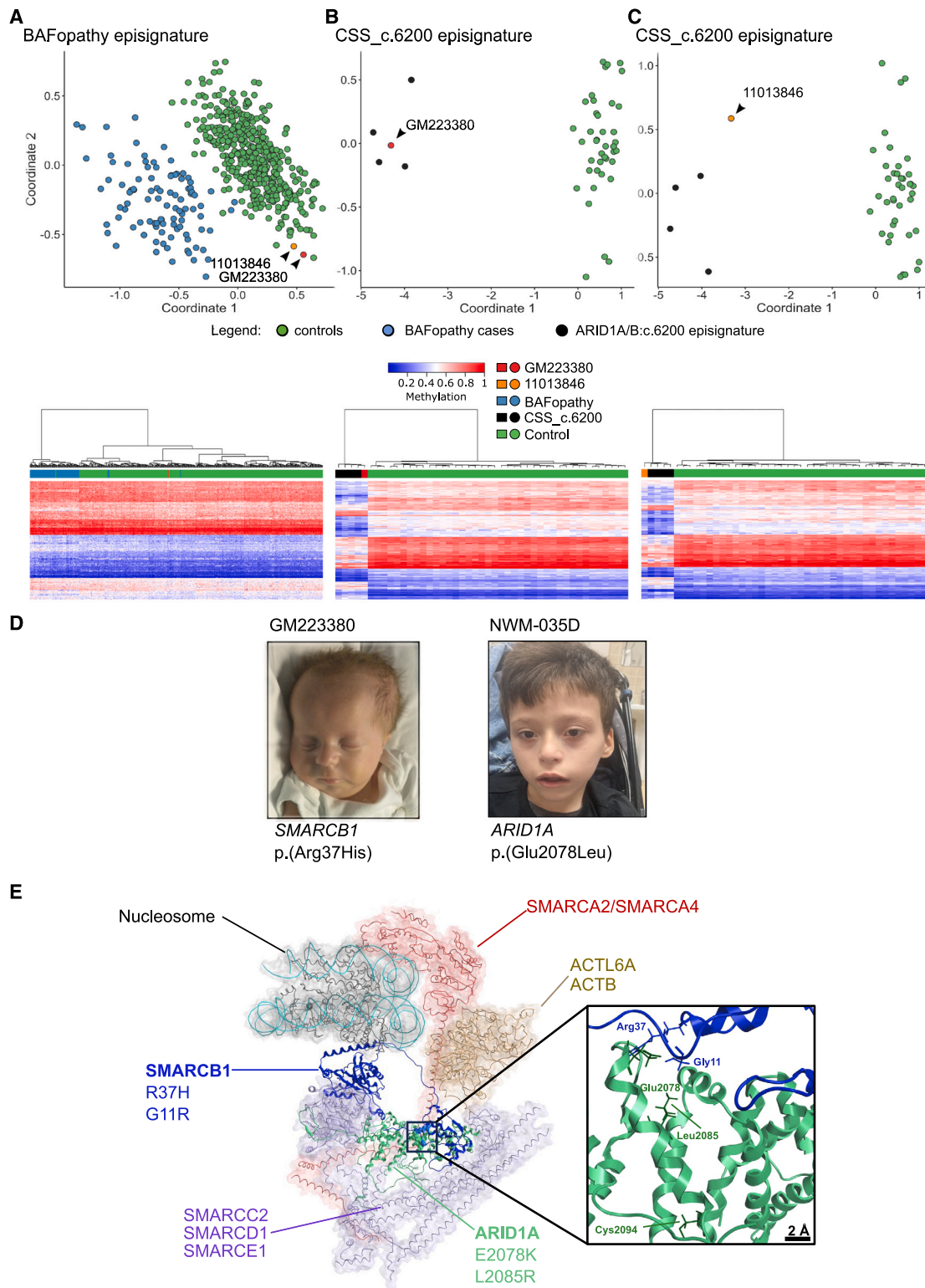


Figure 3. Missense variants in the DNA-binding domain of the SMARCB1 protein reveal a novel rule for the CSS_c.6200 sub-epigenature

(A–C) MDS plots and heatmaps for two subjects with missense variants in *SMARCB1* [GM223380 c.110G>A p.(R37H) and 11013846 c.31G>A p.(G11R)] show their profiles cluster with cases with the CSS_c.6200 sub-domain epigenature, found in individuals with C-terminal variants in *ARID1A* [c.6232G>A p.(E2078K); c.6254T>G p.(L2085R)] and *ARID1B* (c.6133T>C p.(C2045R)).¹⁰

(D) Our two cases with *SMARCB1* p.(R37H) and *ARID1A* p.(E2078L) variants show common facial features with the *SMARCB1* p.(R37H) described patients.³⁰

(legend continued on next page)

although two sub-episignatures specific for regions or variants in *ARID1A*, *ARID1B* and *SMARCA4* have been reported.^{13,21,29} We report here on two cases which add to the current state of the art of the BAFopathies' episignatures.

Samples GM223380 and SMARCB1

This sample was part of the SNV control cohort, from a patient with a subtype of CSS3 (OMIM: 614608) carrying the "Kleefstra" variant, characterized by the recurrent *de novo* *SMARCB1*:c.110G>A p.(R37H) missense substitution. However, the methylation profile did not match the expected broad BAFopathy episignature (Figure 3A), but instead showed a sub-episignature specifically associated with the *ARID1A/B*:c.6200 region identified in cases with missense variants in *ARID1A* (E2078K, L2085R) or *ARID1B* (C2045R) (Figure 3B).¹⁰ The same sub-episignature was observed in a patient with *SMARCB1* G11R present in the EKD (Figure 3C).

We compared the clinical features of our *SMARCB1* R37H patient with the *ARID1A/B*:c.6200 episignature present in our cohort (NMW-35D; *ARID1A* E2078K) (Figure 3D). The clinical similarity of these cases was striking, with common features including severe intellectual disability, choroid plexus hyperplasia, hydrocephalus, walking difficulties, and a typical facial gestalt, in line with their common methylation pattern. To explain this pattern, we visually inspected the BAF complex three-dimensional (3D) protein structure, which showed that *SMARCB1* R37, *SMARCB1* G11, and *ARID1A* (E2078, L2085)/*ARID1B* (C2045) were in close spatial proximity (Figure 3E). We also performed a forcefield-based energy estimation of the mutant *SMARCB1*, *ARID1A*, and *ARID1B* proteins. This computational method estimates the global energy of a protein assembly, yielding indications about the strength of intermolecular interactions within the complexes. The results of the interaction energy estimations suggest that the main effect of the mutations is the overall stabilization of the *SMARCB1*-*ARID1A/B* complex, owing to the formation of novel intermolecular interactions (Figures S6–S10).

Samples GM173400 and SMARCA2

SMARCA2 missense variants cause two distinct syndromes depending on their location within the protein: variants in the catalytic SNF2 ATPase helicase domain cause NCBRS whereas variants outside of this domain cause BIS (Figure 4A). Sample GM173400 was part of the VUS cohort and had a *de novo* *SMARCA2*: c.2566A>G p.(M856V) missense substitution. The patient's phenotype was compatible with BIS (Figures 4B; Table 3), but contrasted with the location of the variant within the SNF2 ATPase domain. The DNAm analysis matched the BIS episignature, which is clearly distinct from that of the BAFopathies (Figure 4C).

We also noted that the mDNA profile of GM173400 (*SMARCA2* M856V) partially overlapped with a previously reported NDD with an underlying *SMARCA4* M886V variant that was noted because its episignature was distinct from that of other *SMARCA4* variants (Figures 4D and 4E). *SMARCA4* M886V was considered a unique example of an episignature that is associated with a specific amino acid change.¹⁰

To explain this observation, alignment of the *SMARCA2* and *SMARCA4* protein sequences showed that *SMARCA2* M856 and *SMARCA4* M886 are positionally homologous amino acids (Figure 5A). This was confirmed by 3D protein homology modeling showing that these amino acids are indeed structural homologues, as is evident when the two protein structures are superposed (Figure 5B). This result supports the hypothesis that an identical M-to-V change in *SMARCA2* at residue M856 or *SMARCA4* at residue M886 exerts equivalent effects resulting in a shared episignatures.

Validation of CNVs of uncertain significance in VCFS/DGS

We analyzed 11 CNVs of uncertain significance that do not span the typical 3-Mb or 1.5-Mb 22q11.21 deletions associated with VCFS/DGS (Figure S11A).^{31,32} Four CNVs consisted of variably sized deletions (approximately 304–772 kb) involving the 3' terminal 22q11.22 VCFS/DGS region. As expected, none of these cases showed the VCFS/DGS profile nor any other known episignature profile (Figures S11B and S11C), confirming that the VCFS/DGS episignature is associated with haploinsufficiency of one or more genes at the 5' end of the critical region. Sample S890 was a possible exception, with a methylation profile that was between VCFS/DGS cases and controls. We hypothesize that this case may have other genetic determinants that cause the DNAm profile to be closer to the VCFS/DGS episignature, also because this deletion is very similar to samples GM203534 and 140901 that have a DNAm profile as the control population. Indeed, S890 has two additional CNVs [GRCh37/hg19:9:127494563-127569992X3; GRCh37/hg19:2:135027917-136083735X3], which may contribute to the DNAm profile.

Finally, we analyzed seven cases with different 22q11.22 distal deletions. None of them showed the VCFS/DGS episignature (Figure S11), including two cases (GM151544 and GM191550) with distal low-copy-number repeat sequence (LCR)-DE deletions that included *TOP3B* (OMIM* 603582), which is associated with cognitive impairment and facial dysmorphisms.³³ Three cases had an embedded deletion within this region, and two cases had distal LCR-EF deletions. In none of these cases did we detect the 22q11.2DS episignature.

(E) Schematic architecture of the human BAFopathy complex. All the variants associated with the CSS_c.6200 sub-domain EpiSign profile encode for amino acids in close spatial proximity of the DNA-binding domain of the *SMARCB1* protein where the R37H and G11R reside. This suggests that the CSS_c.6200 sub-domain episignature depends on a specific alteration in BAF complex function.

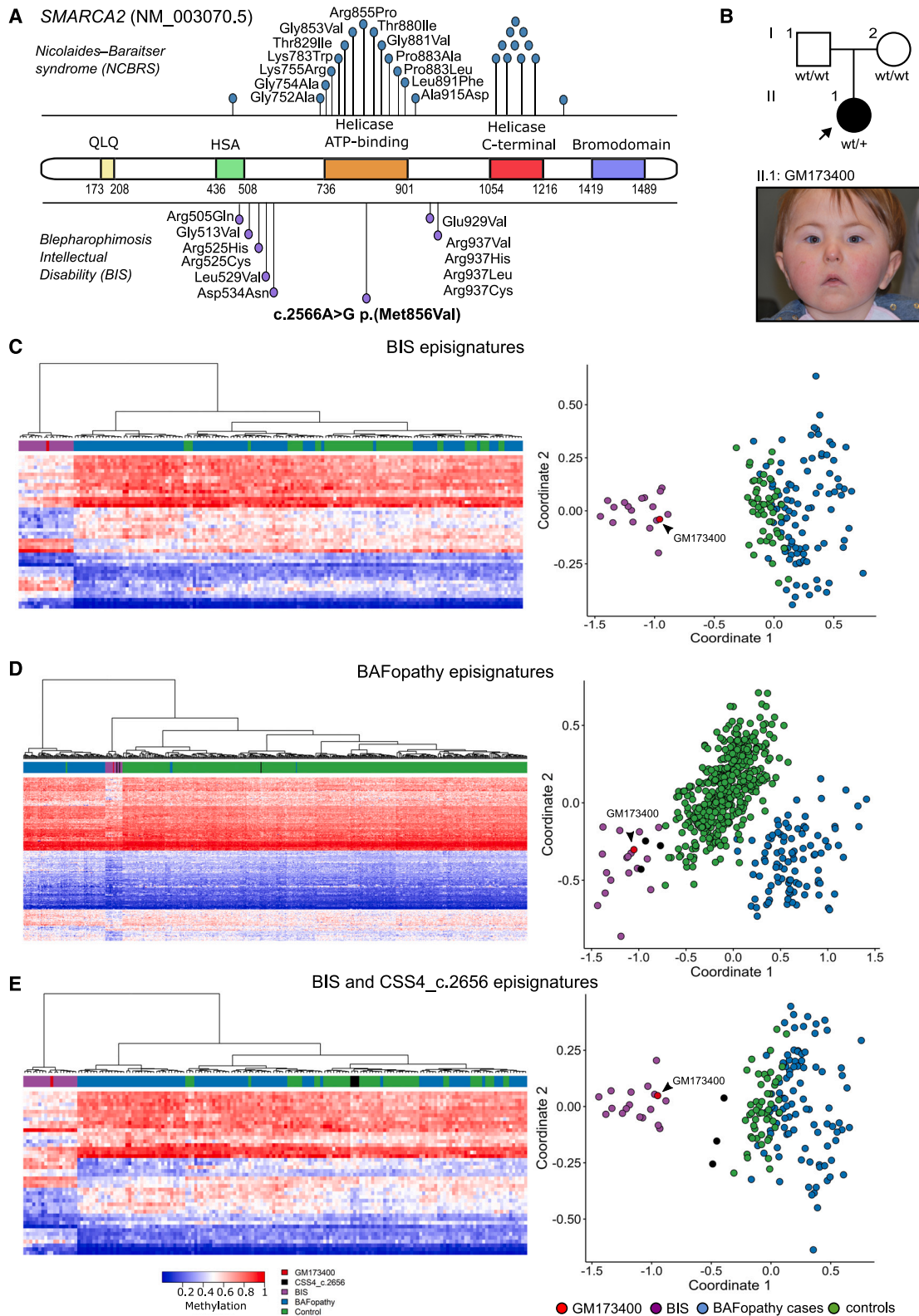


Figure 4. Insights into the distribution of NCBRS/BIS-causative variants

(A) Missense variants in *SMARCA2* cause two different syndromes, depending on their location within the protein. The schematic structure of the *SMARCA2* protein (figure modified from ref.²⁹) shows the five constituent domains with variants associated with NCBRS indicated above the protein and those associated with the BIS below. NCBRS variants cluster in the helicase ATP-binding or helicase C-terminal domains, whereas BIS variants are outside these regions.

(B) Pedigree of case GM173400, who is carrier of a *de novo* *SMARCA2* c.2566A>G p.(M856V) variant. The facial gestalt of GM173400 is compatible with a BIS phenotype.

(legend continued on next page)

Discussion

The use of epigenetic signatures as biomarkers to validate VUS in clinical settings has received significant attention in recent years. Currently, there are more than 65 Mendelian disorders that are defined by specific episignatures.¹⁰ However, there are additional complexities emerging from the interpretation of episignature data. These complexities include (1) broad signals involving genes encoding different proteins that are part of multi-protein complexes; (2) sub-episignatures that are specific to gene protein domains; and (3) even sub-episignatures that are specific to single amino acid changes.¹⁰

VUS pose a challenge in rare genetic conditions, particularly in cases where the clinical presentation is ambiguous. Several cases in our cohort highlight the importance of using an epigenetic classifier to solve VUS. This method allows for the application of the PS3/BS3 functional evidence evaluation criteria within the clinical variant interpretation guidelines of the ACMG/AMP.³⁴

Loss-of-function variants in *ARID1B* are associated with CSS1.³⁵ These variants can include nonsense, frameshift, splice-site, and other deleterious structural changes.^{36,37} However, the role of missense variants in CSS1 is debated; it is suggested that such variants be interpreted with caution and are more likely to be considered harmless.³⁸ Rare missense variants have been reported in the literature and considered pathogenic because they are *de novo*, but without functional evidence to support this assumption.^{38,39} In our study, we identified a *de novo* *ARID1B* missense variant (c.2480C>T p.(A827V)) that was confirmed as pathogenic through episignature analysis, confirming that missense variants in *ARID1B* can indeed cause CSS1. The availability of this rapid test, which can distinguish pathogenic from benign missense changes in *ARID1B*, is an important addition to the tools available for diagnosing CSS1, especially considering that defects in *ARID1B* are the main genetic cause of corpus callosum anomalies in patients with intellectual disability.³⁹

Another example of the discriminating power of episignatures comes from patient NWM-116D with a potentially pathogenic splicing variant in *BRWD3*. Although the clinical presentation was consistent with *BRWD3*-associated intellectual disability, further evaluation was needed to determine if the variant was pathogenic. Splicing variants can be studied using different techniques, such as expression analysis or *in vitro* minigene splicing assays.⁴⁰ In our case, in which patient-derived tissue was unavailable, episignature analysis not only represented a practical means for assessing the impact of the variant, but it also confirmed the pathogenicity of the variant and resolved the case.

Episignature analysis has not only been used to classify patients with VUS, but also to reclassify patients who were initially diagnosed incorrectly or to confirm a clinical suspicion when a predicted causative variant is not detected. In our case, episignature analysis supported the clinical diagnosis in two patients suspected of being CdLS (150163 and NWM-236D), but with no evidence of causative variants in the five genes so far identified as underlying this syndrome. It is known that pathogenic variants in *NIPBL*, *SMC1A*, *SMC3*, *RAD21*, and *HDAC8* explain about 65% of CdLS cases, suggesting that other genes (or variants in non-coding regions) are involved.⁴¹ Data from the literature indicate that deep-intronic and 5' UTR variants in *NIPBL* can also cause CdLS.^{42–46} Therefore, we conducted genome sequencing on case 150163 and thoroughly analyzed the CdLS genes, including introns and non-translated regions, but we could not identify a possible pathogenic variant. This leaves open the possibility of a novel gene causing CdLS. If this hypothesis is true, the novel CdLS gene is likely to encode a protein in the same pathway as the known CdLS genes. Nonetheless, our findings suggest that episignature profiling can be used to support the diagnosis of CdLS even before conducting genetic screening in individuals with a clinical suspicion of CdLS.

In a case of MRXFH1 associated with *ATRX* (111092), episignature analysis also supported the clinical diagnosis despite the absence of any potentially causative single SNV in the gene. This case was further investigated, and ultimately a genomic deletion spanning *ATRX* exons 3–4 was identified, definitively confirming the presence of this disorder.

CNVs represent a significant proportion of the variants that cause NDDs. The changes occurring in DNAm profiles in patients with pathogenic CNVs have not yet been studied systematically, although there are reports of episignatures associated with pathogenic CNVs. In our study, episignature profiling confirmed that all the tested CNVs were indeed pathogenic. The 22q11.2 deletion syndrome is the most common microdeletion syndrome.³² It is characterized by high phenotypic variety and a variety of deletion types and sizes in the 22q11.2 region, which is due to several LCRs (LCR22). A 2.54-Mb deletion is the most common, accounting for approximately 90% of cases. There are also other deletions, such as a 1.5-Mb heterozygous deletion extending from LCR A-B (proximal deletion), a deletion extending from LCR A-C, and smaller atypical (nested) heterozygous deletions extending from LCR B-D or C-D, known as central deletions. Less frequently, distal deletions flanked by LCR D-E and LCR D-F have been reported, which did not show a specific methylation profile.

(C–E) Euclidean hierarchical clustering (heatmap) and MDS plots support the clinical finding showing that GM173400 has a typical BIS episignature, and not a broad BAFopathy one (C), BIS probe set presenting case GM173400 (red), BIS cases (purple), BAFopathy cases (blue), controls (green). (D) BAFopathy probe set presenting case GM173400 (red), BIS cases (purple), CSS4_c.2656 (black), BAFopathy cases (blue), controls (green). (E) BIS probe set presenting case GM173400 (red), BIS cases (purple), CSS4_c.2656 (black), BAFopathy cases (blue), controls (green).

episignatures are associated with a 3D domain and its function. Furthermore, the recurrent SMARCA2 R855P change, which is located just one amino acid upstream of Met856, has been observed in patients with NCBRS and its associated BAF-methylation profile.

It is likely that these episignature-associated domains converge and contribute to a shared function, which ultimately influences the observed phenotypes and methylation patterns. This highlights the importance of considering the 3D organization of proteins and their interactions within complexes when studying the functional impact of amino acid changes and their association with specific signatures.

A final consideration is relative to the methylation profiles determined by variants on the X chromosome. In a female (NWM-024) with mild Borjeson-Forssman-Lehmann syndrome,^{27,48,49} associated with *de novo* PHF6 p.(C297F),¹⁷ we did not find the expected PHF6 episignature. We suggest that this gene has sex-related episignature depending on whether female or male patients are analyzed. In fact, patients used to generate the episignature for PHF6 were only males. Alternatively, a domain-specific episignature may exist since our patient's change resides in the PHD2 domain where all reported missense variants in females are located (Figure S3). The role of skewed XCI in determining the epigenetic profile should also be considered as female cases with CdLS5 (OMIM: 300882) (*HDAC8* gene) with completely skewed X-inactivation did not show any change in their methylation profile.⁹

This interplay between an X-linked condition and episignatures could be also observed in another family where the *KDM5C* p.(D402N) change segregated in a mildly affected male, and two unaffected females. Notably, codon 402 has been reported to be changed to Tyr in other MRXSJ patients and experimentally confirmed as deleterious.⁵⁰ We have previously examined this family using XCI and linkage analysis¹⁷ and we showed that the mother tended to inactivate the mutant allele, while the affected sister had the wild type allele. Methylation analysis in the male proband 121116 computed an MVP score of 0.71, suggesting on a DNAm profile more similar to carrier females than affected males; his sister 121886 had an MVP of 0.54 with a DNAm profile similar to carrier females; and the carrier mother 121888 had an MVP score of 0.11, i.e., with a methylation profile like that of the control population, overall suggesting the variant is hypomorphic, and XCI is modulating the DNAm profile influencing protein levels. These findings are in line with the reported linear relationship seen between the dosage of the defective protein and the intensity of DNAm alterations in other syndromes, such as immunodeficiency-centromeric instability-facial anomalies syndrome types 2–4 (ICF2–4).⁹

Patient NWM-021D had an unusual finding with skewed XCI and DNAm pattern, which corresponds with two non X-linked genes, *ANKRD11* (KBG) (OMIM: 148050) and *SETD5* (MRD23) (OMIM: 615761). From a clinical perspective, the patient does not perfectly match with either of

these conditions. However, the literature suggests that *ANKRD11* is a more likely candidate due to the involvement of its protein in XCI, specifically its interaction with HDAC3, a component of the XCI mechanism.^{51,52} It is also interesting to note that KBG is more common in males (male to female ratio 21:8) and initially it was proposed that *ANKRD11* had an X-linked inheritance.^{53,54} It would thus be of great interest to investigate how many autosomal genes play a role in XCI and how this may impact episignature interpretation.

Conclusions

Using the EpiSign v.3 classifier we have highlighted the role of episignatures in solving VUS within a cohort of NDD cases. The integrated EpiSign/ES approach was helpful for re-evaluating already solved cases, for reclassifying variants of dubious clinical significance, and for detecting underlying genetic causes. Finally, we provide novel insights into sub-domain episignatures of the BAF complex, showing that they correlate with 3D functional domains. Despite current limitations of the size of its gene catalog, the EpiSign classifier is a powerful addition to the geneticist's armamentarium, capable of obtaining returnable genetic results, especially in NDD patients.

Data and code availability

The data supporting the findings of this study are available from the corresponding author. All variants have been deposited into ClinVar (SUB13925176); variants were validated with Variant Validator.

Some of the datasets used in this study are publicly available and may be obtained from the gene expression omnibus (GEO) using the following accession numbers: GEO: GSE116992, GSE66552, GSE74432, GSE97362, GSE116300, GSE95040, GSE104451, GSE125367, GSE55491, GSE108423, GSE116300, GSE89353, GSE52588, GSE42861, GSE85210, GSE87571, GSE87648, GSE99863, and GSE35069. These include DNAm data from patients with Kabuki syndrome, Sotos syndrome, CHARGE syndrome, immunodeficiency-centromeric ICF syndrome, Williams-Beuren syndrome, Chr7q11.23 duplication syndrome, BAFopathies, Down syndrome, a large cohort of unresolved subjects with developmental delays and congenital abnormalities, and several large cohorts of DNAm data from the general population. The rest of the data including the FA samples are not available due to the institutional or REB restrictions. EpiSign is a proprietary, trademarked analytical software owned by EpiSign Inc. Parts of it are based on the methods and publicly available software that are referenced in the Methods.

Supplemental information

Supplemental information can be found online at <https://doi.org/10.1016/j.xhgg.2024.100309>.

Acknowledgments

We are grateful to patients and their families who collaborated in this study.

Funding: This research received funding from the European Union-NextGeneration EU PNRR-MR1-2022-12376067 “Multiomic strategies to implement the diagnostic workflow of rare diseases” -Settore di afferenza 56209 - nell’ambito del bando nell’ambito della Missione M6/componente: C2 Investimento: 2.1 “Valorizzazione e potenziamento della ricerca biomedica del SSN” del Piano nazionale di Ripresa e Resilienza (PNRR) CUP G13C22001390001; from the Italian Ministry for Education, University and Research (Ministero dell’Istruzione, dell’Università e della Ricerca - MIUR) PRIN2020 code 20203P8C3X to A.B.; from the Fondazione Cassa di Risparmio di Torino to A.B.; from the MIUR project “Dipartimenti di Eccellenza 2023-2027” to the Department of Neurosciences “Rita Levi Montalcini” (University of Turin). This study was also supported by the NIHR Manchester Biomedical Research Centre (NIHR203308).

Author contributions

Conceptualization: S.T., A.B., and B.S.; data collection and analysis: S.T., J.K., M.R.S., L.P., C.G., D.C., E.D.G., R.M., G.M., F.P., S.Carestiato, S.Cardaropoli, V.P., A.R., E.G., T.P., P.D., J.R., K.R., H.M.C., A.P., B.P., E.S., C.C., K.M., S.J., S.B., A.M., and G.B.E.; data curation: J.K. and J.R.; investigation: S.T., J.K., and J.R.; supervision: S.T., E.F., B.S., A.B., and S.B.; writing – original draft: S.T., E.F., and A.B.; writing – review and editing: all authors.

Declaration of interests

B.S. is a shareholder in EpiSign Inc, company involved in commercialization of EpiSign technology.

Received: December 6, 2023

Accepted: May 7, 2024

Web resources

AlphaFold DB (<https://alphafold.ebi.ac.uk>) was employed for the retrieval of full-length predicted protein structures. Templates for the models of the human protein complexes were retrieved from the Protein DataBank (<https://www.rcsb.org>). Preliminary analysis of contact residues was performed with the webserver PDBSum Generate (<https://www.ebi.ac.uk/thornton-srv/databases/pdbsum/Generate.html>). Last access to the webserver and database: June 2nd, 2023. EpiSign v.3: <https://episign.lhsc.on.ca/>.

References

- Parenti, I., Rabaneda, L.G., Schoen, H., and Novarino, G. (2020). Neurodevelopmental Disorders: From Genetics to Functional Pathways. *Trends Neurosci.* *43*, 608–621. <https://doi.org/10.1016/j.tins.2020.05.004>.
- van der Sanden, B.P.G.H., Schobers, G., Corominas Galbany, J., Koolen, D.A., Sinnema, M., van Reeuwijk, J., Stumpel, C.T.R.M., Kleefstra, T., de Vries, B.B.A., Ruitkamp-Versteeg, M., et al. (2023). The performance of genome sequencing as a first-tier test for neurodevelopmental disorders. *Eur. J. Hum. Genet.* *31*, 81–88. <https://doi.org/10.1038/s41431-022-01185-9>.
- 100000 Genomes Project Pilot Investigators, Smedley, D., Smith, K.R., Martin, A., Thomas, E.A., McDonagh, E.M., Cipriani, V., Ellingford, J.M., Arno, G., Tucci, A., et al. (2021). 100,000 Genomes Pilot on Rare-Disease Diagnosis in Health Care - Preliminary Report. *N. Engl. J. Med.* *385*, 1868–1880. <https://doi.org/10.1056/NEJMoa2035790>.
- Manickam, K., McClain, M.R., Demmer, L.A., Biswas, S., Kearney, H.M., Malinowski, J., Massingham, L.J., Miller, D., Yu, T.W., Hisama, F.M.; and ACMG Board of Directors (2021). Exome and genome sequencing for pediatric patients with congenital anomalies or intellectual disability: an evidence-based clinical guideline of the American College of Medical Genetics and Genomics (ACMG). *Genet. Med.* *23*, 2029–2037. <https://doi.org/10.1038/s41436-021-01242-6>.
- Hartley, T., Lemire, G., Kernohan, K.D., Howley, H.E., Adams, D.R., and Boycott, K.M. (2020). New Diagnostic Approaches for Undiagnosed Rare Genetic Diseases. *Annu. Rev. Genomics Hum. Genet.* *21*, 351–372. <https://doi.org/10.1146/annurev-genom-083118-015345>.
- Sadikovic, B., Aref-Eshghi, E., Levy, M.A., and Rodenhiser, D. (2019). DNA methylation signatures in mendelian developmental disorders as a diagnostic bridge between genotype and phenotype. *Epigenomics* *11*, 563–575. <https://doi.org/10.2217/epi-2018-0192>.
- Bjornsson, H.T. (2015). The Mendelian disorders of the epigenetic machinery. *Genome Res.* *25*, 1473–1481. <https://doi.org/10.1101/gr.190629.115>.
- Sadikovic, B., Levy, M.A., Kerkhof, J., Aref-Eshghi, E., Schenkel, L., Stuart, A., McConkey, H., Henneman, P., Venema, A., Schwartz, C.E., et al. (2021). Clinical epigenomics: genome-wide DNA methylation analysis for the diagnosis of Mendelian disorders. *Genet. Med.* *23*, 1065–1074. <https://doi.org/10.1038/s41436-020-01096-4>.
- Aref-Eshghi, E., Kerkhof, J., Pedro, V.P., Groupe DI France, Barat-Houari, M., Ruiz-Pallares, N., Andrau, J.C., Lacombe, D., Van-Gils, J., Fergelot, P., et al. (2020). Evaluation of DNA Methylation Episignatures for Diagnosis and Phenotype Correlations in 42 Mendelian Neurodevelopmental Disorders. *Am. J. Hum. Genet.* *106*, 356–370. <https://doi.org/10.1016/j.ajhg.2020.01.019>.
- Levy, M.A., McConkey, H., Kerkhof, J., Barat-Houari, M., Bargiacchi, S., Biamino, E., Bralo, M.P., Cappuccio, G., Ciolfi, A., Clarke, A., et al. (2022). Novel diagnostic DNA methylation episignatures expand and refine the epigenetic landscapes of Mendelian disorders. *HGG Adv.* *3*, 100075. <https://doi.org/10.1016/j.xhgg.2021.100075>.
- Schreyer, L., Reilly, J., McConkey, H., Kerkhof, J., Levy, M.A., Hu, J., Hnaini, M., Sadikovic, B., and Campbell, C. (2023). The discovery of the DNA methylation episignature for Duchenne muscular dystrophy. *Neuromuscul. Disord.* *33*, 5–14. <https://doi.org/10.1016/j.nmd.2022.12.003>.
- Bogaert, E., Garde, A., Gautier, T., Rooney, K., Duffourd, Y., LeBlanc, P., van Reempts, E., Tran Mau-Them, F., Wentzensen, I.M., Au, K.S., et al. (2023). SRSF1 haploinsufficiency is responsible for a syndromic developmental disorder associated with intellectual disability. *Am. J. Hum. Genet.* *110*, 790–808. <https://doi.org/10.1016/j.ajhg.2023.03.016>.
- Aref-Eshghi, E., Bend, E.G., Hood, R.L., Schenkel, L.C., Carere, D.A., Chakrabarti, R., Nagamani, S.C.S., Cheung, S.W., Campeau, P.M., Prasad, C., et al. (2018). BAFOpathies’ DNA

- methylation epi-signatures demonstrate diagnostic utility and functional continuum of Coffin-Siris and Nicolaides-Baraitser syndromes. *Nat. Commun.* 9, 4885. <https://doi.org/10.1038/s41467-018-07193-y>.
14. Bend, E.G., Aref-Eshghi, E., Everman, D.B., Rogers, R.C., Cathey, S.S., Prijoles, E.J., Lyons, M.J., Davis, H., Clarkson, K., Gripp, K.W., et al. (2019). Gene domain-specific DNA methylation epigenotypes highlight distinct molecular entities of ADNP syndrome. *Clin. Epigenetics* 11, 64. <https://doi.org/10.1186/s13148-019-0658-5>.
 15. Rooney, K., and Sadikovic, B. (2022). DNA Methylation Episignatures in Neurodevelopmental Disorders Associated with Large Structural Copy Number Variants: Clinical Implications. *Int. J. Mol. Sci.* 23, 7862. <https://doi.org/10.3390/ijms23147862>.
 16. van der Laan, L., Rooney, K., Trooster, T.M., Mannens, M.M., Sadikovic, B., and Henneman, P. (2022). DNA methylation episignatures: insight into copy number variation. *Epigenomics* 14, 1373–1388. <https://doi.org/10.2217/epi-2022-0287>.
 17. Giovenino, C., Trajkova, S., Pavinato, L., Cardaropoli, S., Pullano, V., Ferrero, E., Sukarova-Angelovska, E., Carestiato, S., Salmin, P., Rinninella, A., et al. (2023). Skewed X-chromosome inactivation in unsolved neurodevelopmental disease cases can guide re-evaluation For X-linked genes. *Eur. J. Hum. Genet.* 31, 1228–1236. <https://doi.org/10.1038/s41431-023-01324-w>.
 18. Li, Q., and Wang, K. (2017). InterVar: Clinical Interpretation of Genetic Variants by the 2015 ACMG-AMP Guidelines. *Am. J. Hum. Genet.* 100, 267–280. <https://doi.org/10.1016/j.ajhg.2017.01.004>.
 19. Riggs, E.R., Andersen, E.F., Cherry, A.M., Kantarci, S., Kearney, H., Patel, A., Raca, G., Ritter, D.I., South, S.T., Thorland, E.C., et al. (2020). Technical standards for the interpretation and reporting of constitutional copy-number variants: a joint consensus recommendation of the American College of Medical Genetics and Genomics (ACMG) and the Clinical Genome Resource (ClinGen). *Genet. Med.* 22, 245–257. <https://doi.org/10.1038/s41436-019-0686-8>.
 20. Richards, S., Aziz, N., Bale, S., Bick, D., Das, S., Gastier-Foster, J., Grody, W.W., Hegde, M., Lyon, E., Spector, E., et al. (2015). Standards and guidelines for the interpretation of sequence variants: a joint consensus recommendation of the American College of Medical Genetics and Genomics and the Association for Molecular Pathology. *Genet. Med.* 17, 405–424. <https://doi.org/10.1038/gim.2015.30>.
 21. Levy, M.A., Relator, R., McConkey, H., Pranckeviciene, E., Kerkhof, J., Barat-Houari, M., Bargiacchi, S., Biamino, E., Palomares Bralo, M., Cappuccio, G., et al. (2022). Functional correlation of genome-wide DNA methylation profiles in genetic neurodevelopmental disorders. *Hum. Mutat.* 43, 1609–1628. <https://doi.org/10.1002/humu.24446>.
 22. Kerkhof, J., Squeo, G.M., McConkey, H., Levy, M.A., Piemontese, M.R., Castori, M., Accadia, M., Biamino, E., Della Monica, M., Di Giacomo, M.C., et al. (2022). DNA methylation episignature testing improves molecular diagnosis of Mendelian chromatinopathies. *Genet. Med.* 24, 51–60. <https://doi.org/10.1016/j.gim.2021.08.007>.
 23. He, S., Wu, Z., Tian, Y., Yu, Z., Yu, J., Wang, X., Li, J., Liu, B., and Xu, Y. (2020). Structure of nucleosome-bound human BAF complex. *Science* 367, 875–881. <https://doi.org/10.1126/science.aaz9761>.
 24. Ponder, J.W., and Case, D.A. (2003). Force fields for protein simulations. *Adv. Protein Chem.* 66, 27–85. [https://doi.org/10.1016/s0065-3233\(03\)66002-x](https://doi.org/10.1016/s0065-3233(03)66002-x).
 25. de Goede, C., Yue, W.W., Yan, G., Ariyaratnam, S., Chandler, K.E., Downes, L., Khan, N., Mohan, M., Lowe, M., and Banka, S. (2016). Role of reverse phenotyping in interpretation of next generation sequencing data and a review of INPP5E related disorders. *Eur. J. Paediatr. Neurol.* 20, 286–295. <https://doi.org/10.1016/j.ejpn.2015.11.012>.
 26. Li, D., Ahrens-Nicklas, R.C., Baker, J., Bhambhani, V., Calhoun, A., Cohen, J.S., Deardorff, M.A., Fernández-Jaén, A., Kamien, B., Jain, M., et al. (2020). The variability of SMARCA4-related Coffin-Siris syndrome: Do nonsense candidate variants add to milder phenotypes? *Am. J. Med. Genet.* 182, 2058–2067. <https://doi.org/10.1002/ajmg.a.61732>.
 27. Gerber, C.B., Fliedner, A., Bartsch, O., Berland, S., Dewenter, M., Haug, M., Hayes, I., Marin-Reina, P., Mark, P.R., Martinez-Castellano, F., et al. (2022). Further characterization of Borjeson-Forsman-Lehmann syndrome in females due to de novo variants in PHF6. *Clin. Genet.* 102, 182–190. <https://doi.org/10.1111/cge.14173>.
 28. Valencia, A.M., Sankar, A., van der Sluijs, P.J., Satterstrom, F.K., Fu, J., Talkowski, M.E., Vergano, S.A.S., Santen, G.W.E., and Kadoch, C. (2023). Landscape of mSWI/SNF chromatin remodeling complex perturbations in neurodevelopmental disorders. *Nat. Genet.* 55, 1400–1412. <https://doi.org/10.1038/s41588-023-01451-6>.
 29. Cappuccio, G., Sayou, C., Tanno, P.L., Tisserant, E., Bruel, A.L., Kennani, S.E., Sá, J., Low, K.J., Dias, C., Havlovicová, M., et al. (2020). De novo SMARCA2 variants clustered outside the helicase domain cause a new recognizable syndrome with intellectual disability and blepharophimosis distinct from Nicolaides-Baraitser syndrome. *Genet. Med.* 22, 1838–1850. <https://doi.org/10.1038/s41436-020-0898-y>.
 30. Diets, I.J., Prescott, T., Champaigne, N.L., Mancini, G.M.S., Krossnes, B., Frič, R., Kocsis, K., Jongmans, M.C.J., and Kleefstra, T. (2019). A recurrent de novo missense pathogenic variant in SMARCB1 causes severe intellectual disability and choroid plexus hyperplasia with resultant hydrocephalus. *Genet. Med.* 21, 572–579. <https://doi.org/10.1038/s41436-018-0079-4>.
 31. Rooney, K., Levy, M.A., Haghshenas, S., Kerkhof, J., Rogaia, D., Tedesco, M.G., Imperatore, V., Mencarelli, A., Squeo, G.M., Di Venere, E., et al. (2021). Identification of a DNA Methylation Episignature in the 22q11.2 Deletion Syndrome. *Int. J. Mol. Sci.* 22, 8611. <https://doi.org/10.3390/ijms22168611>.
 32. McDonald-McGinn, D.M., Sullivan, K.E., Marino, B., Philip, N., Swillen, A., Vorstman, J.A.S., Zackai, E.H., Emanuel, B.S., Vermeesch, J.R., Morrow, B.E., et al. (2015). 22q11.2 deletion syndrome. *Nat. Rev. Dis. Primers* 1, 15071. <https://doi.org/10.1038/nrdp.2015.71>.
 33. Kaufman, C.S., Genovese, A., and Butler, M.G. (2016). Deletion of TOP3B Is Associated with Cognitive Impairment and Facial Dysmorphism. *Cytogenet. Genome Res.* 150, 106–111. <https://doi.org/10.1159/000452815>.
 34. Brnich, S.E., Abou Tayoun, A.N., Couch, F.J., Cutting, G.R., Greenblatt, M.S., Heinen, C.D., Kanavy, D.M., Luo, X., McNulty, S.M., Starita, L.M., et al. (2019). Recommendations for application of the functional evidence PS3/BS3 criterion using the ACMG/AMP sequence variant interpretation framework. *Genome Med.* 12, 3. <https://doi.org/10.1186/s13073-019-0690-2>.
 35. Tsurusaki, Y., Okamoto, N., Ohashi, H., Kosho, T., Imai, Y., Hibi-Ko, Y., Kaname, T., Naritomi, K., Kawame, H., Wakui, K., et al. (2012). Mutations affecting components of the

- SWI/SNF complex cause Coffin-Siris syndrome. *Nat. Genet.* 44, 376–378. <https://doi.org/10.1038/ng.2219>.
36. Moffat, J.J., Smith, A.L., Jung, E.M., Ka, M., and Kim, W.Y. (2022). Neurobiology of ARID1B haploinsufficiency related to neurodevelopmental and psychiatric disorders. *Mol. Psychiatry* 27, 476–489. <https://doi.org/10.1038/s41380-021-01060-x>.
 37. van der Sluijs, P.J., Jansen, S., Vergano, S.A., Adachi-Fukuda, M., Alanay, Y., AlKindy, A., Baban, A., Bayat, A., Beck-Wödl, S., Berry, K., et al. (2019). The ARID1B spectrum in 143 patients: from nonsyndromic intellectual disability to Coffin-Siris syndrome. *Genet. Med.* 21, 1295–1307. <https://doi.org/10.1038/s41436-018-0330-z>.
 38. Mignot, C., Moutard, M.L., Rastetter, A., Boutaud, L., Heide, S., Bilette, T., Doummar, D., Garel, C., Afenjar, A., Jacquette, A., et al. (2016). ARID1B mutations are the major genetic cause of corpus callosum anomalies in patients with intellectual disability. *Brain* 139, e64. <https://doi.org/10.1093/brain/aww181>.
 39. Yu, Y., Yao, R., Wang, L., Fan, Y., Huang, X., Hirschhorn, J., Dauber, A., and Shen, Y. (2015). De novo mutations in ARID1B associated with both syndromic and non-syndromic short stature. *BMC Genom.* 16, 701. <https://doi.org/10.1186/s12864-015-1898-1>.
 40. Lord, J., and Baralle, D. (2021). Splicing in the Diagnosis of Rare Disease: Advances and Challenges. *Front. Genet.* 12, 689892. <https://doi.org/10.3389/fgene.2021.689892>.
 41. Woods, S.A., Robinson, H.B., Kohler, L.J., Agamanolis, D., Sterbenz, G., and Khalifa, M. (2014). Exome sequencing identifies a novel EP300 frame shift mutation in a patient with features that overlap Cornelia de Lange syndrome. *Am. J. Med. Genet.* 164A, 251–258. <https://doi.org/10.1002/ajmg.a.36237>.
 42. Coursimault, J., Cassinari, K., Lecoquierre, F., Quenez, O., Coutant, S., Derambure, C., Vezain, M., Drouot, N., Vera, G., Schaefer, E., et al. (2022). Deep intronic NIPBL de novo mutations and differential diagnoses revealed by whole genome and RNA sequencing in Cornelia de Lange syndrome patients. *Hum. Mutat.* 43, 1882–1897. <https://doi.org/10.1002/humu.24438>.
 43. Krawczynska, N., Wierzba, J., Jasiński, J., and Wasag, B. (2019). Molecular characterization of two novel intronic variants of NIPBL gene detected in unrelated Cornelia de Lange syndrome patients. *BMC Med. Genet.* 20, 1. <https://doi.org/10.1186/s12881-018-0738-y>.
 44. Seyama, R., Uchiyama, Y., Ceroni, J.R.M., Kim, V.E.H., Furquim, I., Honjo, R.S., Castro, M.A.A., Pires, L.V.L., Aoi, H., Iwama, K., et al. (2022). Pathogenic variants detected by RNA sequencing in Cornelia de Lange syndrome. *Genomics* 114, 110468. <https://doi.org/10.1016/j.ygeno.2022.110468>.
 45. Chen, Y., Chen, Q., Yuan, K., Zhu, J., Fang, Y., Yan, Q., and Wang, C. (2022). A Novel de Novo Variant in 5' UTR of the. *Genes* 13, 740. <https://doi.org/10.3390/genes13050740>.
 46. Coursimault, J., Rovelet-Lecrux, A., Cassinari, K., Brischoux-Boucher, E., Saugier-veber, P., Goldenberg, A., Lecoquierre, F., Drouot, N., Richard, A.C., Vera, G., et al. (2022). uORF-introducing variants in the 5'UTR of the NIPBL gene as a cause of Cornelia de Lange syndrome. *Hum. Mutat.* 43, 1239–1248. <https://doi.org/10.1002/humu.24384>.
 47. White-Brown, A., Choufani, S., Care4Rare Canada Consortium, Weksberg, R., and Dymont, D. (2023). Missense variant in SRCAP with distinct DNA methylation signature associated with non-FLHS SRCAP-related neurodevelopmental disorder. *Am. J. Med. Genet.* 191, 2640–2646. <https://doi.org/10.1002/ajmg.a.63329>.
 48. Zweier, C., Kraus, C., Brueton, L., Cole, T., Degenhardt, F., Engels, H., Gillissen-Kaesbach, G., Graul-Neumann, L., Horn, D., Hoyer, J., et al. (2013). A new face of Borjeson-Forsman-Lehmann syndrome? De novo mutations in PHF6 in seven females with a distinct phenotype. *J. Med. Genet.* 50, 838–847. <https://doi.org/10.1136/jmedgenet-2013-101918>.
 49. Wieczorek, D., Bögershausen, N., Beleggia, F., Steiner-Haldenstätter, S., Pohl, E., Li, Y., Milz, E., Martin, M., Thiele, H., Altmüller, J., et al. (2013). A comprehensive molecular study on Coffin-Siris and Nicolaidis-Baraitser syndromes identifies a broad molecular and clinical spectrum converging on altered chromatin remodeling. *Hum. Mol. Genet.* 22, 5121–5135. <https://doi.org/10.1093/hmg/ddt366>.
 50. Brookes, E., Laurent, B., Öunap, K., Carroll, R., Moeschler, J.B., Field, M., Schwartz, C.E., Gecz, J., and Shi, Y. (2015). Mutations in the intellectual disability gene KDM5C reduce protein stability and demethylase activity. *Hum. Mol. Genet.* 24, 2861–2872. <https://doi.org/10.1093/hmg/ddv046>.
 51. Chaves, L.D., Carvalho, L.M.L., Tolezano, G.C., Pires, S.F., Costa, S.S., de Scliar, M.O., Giuliani, L.d.R., Bertola, D.R., Santos-Rebouças, C.B., Seo, G.H., et al. (2023). Skewed X-chromosome Inactivation in Women with Idiopathic Intellectual Disability is Indicative of Pathogenic Variants. *Mol. Neurobiol.* 60, 3758–3769. <https://doi.org/10.1007/s12035-023-03311-0>.
 52. Żylicz, J.J., Bousard, A., Žumer, K., Dossin, F., Mohammad, E., da Rocha, S.T., Schwalb, B., Syx, L., Dingli, F., Loew, D., et al. (2019). The Implication of Early Chromatin Changes in X Chromosome Inactivation. *Cell* 176, 182–197.e123. <https://doi.org/10.1016/j.cell.2018.11.041>.
 53. Maegawa, G.H.B., Leite, J.C.L., Félix, T.M., da Silveira, H.L.D., and da Silveira, H.E. (2004). Clinical variability in KBG syndrome: report of three unrelated families. *Am. J. Med. Genet.* 131, 150–154. <https://doi.org/10.1002/ajmg.a.30293>.
 54. Brancati, F., D'Avanzo, M.G., Digilio, M.C., Sarkozy, A., Biondi, M., De Brasi, D., Mingarelli, R., and Dallapiccola, B. (2004). KBG syndrome in a cohort of Italian patients. *Am. J. Med. Genet.* 131, 144–149. <https://doi.org/10.1002/ajmg.a.30292>.

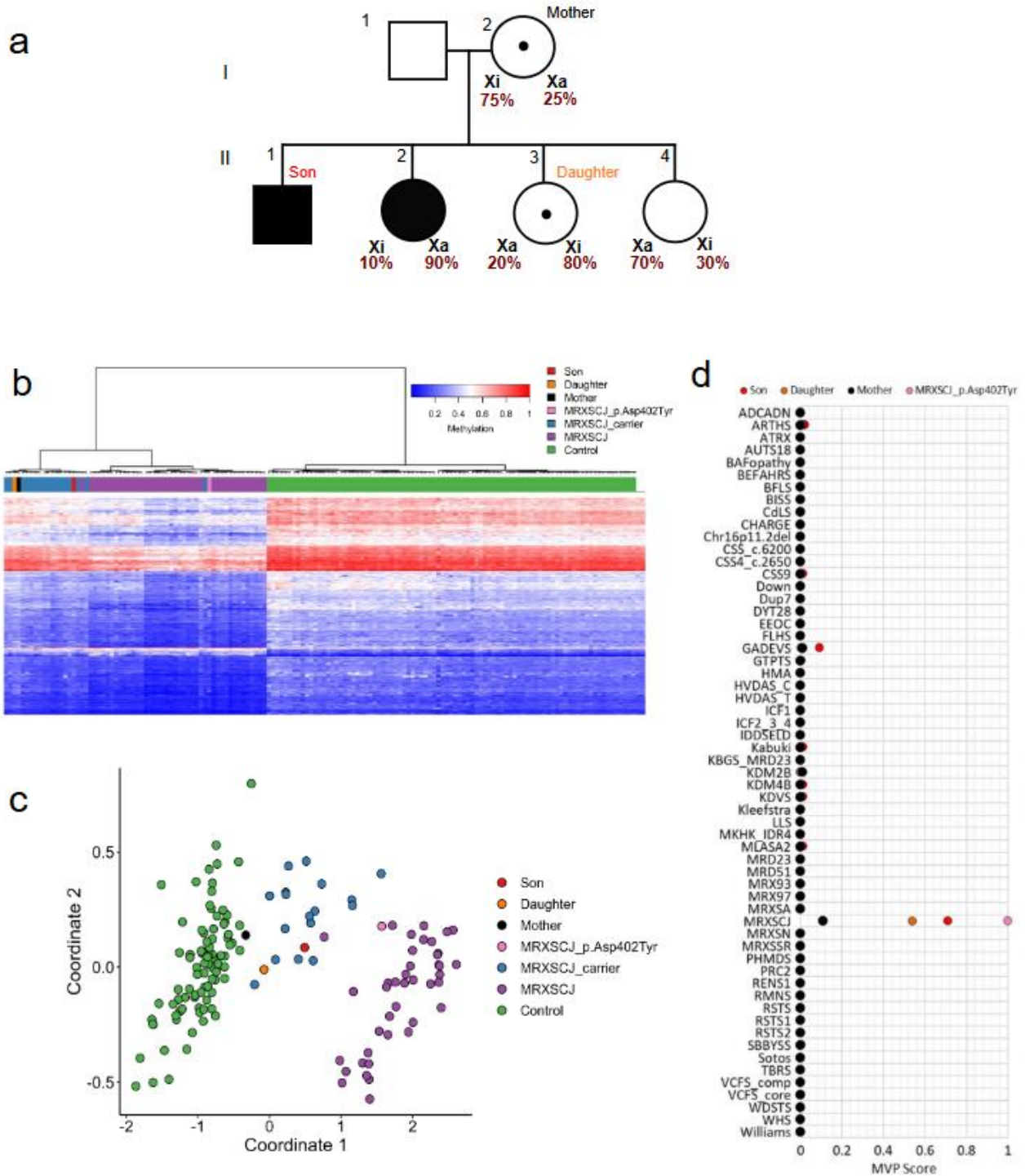
Supplemental information

DNA methylation analysis in patients with neurodevelopmental disorders improves variant interpretation and reveals complexity

Slavica Trajkova, Jennifer Kerkhof, Matteo Rossi Sebastiano, Lisa Pavinato, Enza Ferrero, Chiara Giovenino, Diana Carli, Eleonora Di Gregorio, Roberta Marinoni, Giorgia Mandrile, Flavia Palermo, Silvia Carestiato, Simona Cardaropoli, Verdiana Pullano, Antonina Rinninella, Elisa Giorgio, Tommaso Pippucci, Paola Dimartino, Jessica Rzas, Kathleen Rooney, Haley McConkey, Aleksandar Petlichkovski, Barbara Pasini, Elena Sukarova-Angelovska, Christopher M. Campbell, Kay Metcalfe, Sarah Jenkinson, Siddharth Banka, Alessandro Mussa, Giovanni Battista Ferrero, Bekim Sadikovic, and Alfredo Brusco

SUPPLEMENTAL INFORMATION

- **Supplemental figures S1-S11**
- **Supplemental tables 1-3**
- **Supplemental Materials and methods**
- **Supplemental References**



Supplemental figure S1. Family tree of *KDM5C* cases and EpiSign analysis

Panel a. Family tree and X-chromosome inactivation analysis (for further details please see¹). **Panel b.** Euclidean hierarchical clustering (heatmap) of MRXSCJ-male cases (purple), MRXSCJ-female carriers (blue), green (controls); red-son (II-1); orange-daughter (II-3), black-mother (I-2) pink-male case MRXSCJ: p.(D402Y). **Panel c.** Multidimensional scaling (MDS) plot presents the differentiation of MRXSCJ-male cases (purple), MRXSCJ-female carriers (blue), green (controls); red-son (II-1); orange-daughter (II-3), black-mother (I-2); pink-male case MRXSCJ: p.(D402Y). **Panel d-**MVP score plots orange-daughter (II-3), black-mother (I-2), red-son (II-1); pink-male case MRXSCJ:p.(D402Y).

Alignments :

73.9% identity in 1672 residues overlap; Score: 5747.0; Gap frequency: 6.5%

```
P51531|SMC      1 MSTPTDP-GAMPHPGSPGPGSPGPI LGSPGPGSPGSPG SVHSMGPPSPGPPSVSHPMPT
P51532|SMC      1 MSTPDPFLGGTTPRPGSPGPGSPGAM LGSPGPG--SPGSAHSMGPPSPGPPSAGHPIPT
      **** * * * ***** ***** * * * * * * * * * * * * * * * * * * * *

P51531|SMC     60 MGSTDFPQEGMHQMHKPIDGIHDKGIVEDIHCGSMKGTGMRPP-HPGMGFPQSPMDQHSQ
P51532|SMC     59 QGPGGYPQDNMHQMHKPMESMHEKGM SDDPRYNQMKGMGMRSGGHAGMPPSPMDQHSQ
      *   ** ***** * * * * * * * * * * * * * * * * * * * *

P51531|SMC    119 GYMSPHPSPLGAPEHVSSPMSGGGPTP-PQMPPSQPGALIPG-DPQAMSQPNRGSPFSP
P51532|SMC    119 GY----PSPLGGSEHASSVPASGSPSGPQMSSGGGAPLDGADPQALGQQNRGPTPFNQ
      **   ***** ** *** * * * * * * * * * * * * * * * * * * * *

P51531|SMC    177 VQLHQLRAQILAYKMLARGQPLPETLQLAVQGKRTLPLGLQQQQQQQQQQQQ-----
P51532|SMC    175 NQLHQLRAQIMAYKMLARGQPLPDHLQMAVQGKRPMPGMQQQMPTLPPPSVSATGPGPGP
      ***** ***** * * * * * * * * * * * * * * * * * * * *

P51531|SMC    229 -----QQQQQQQQQQPQQPPQPT----QQQQPALVNYNRPSGPGPELSG
P51532|SMC    235 GPGPGPGPPAPPNYSRPHGMGPNMPPGPGSGVPPGMPGQPPGGPKPWPEGPMANAAA
      *   * * * * * * * * * * * * * * * * * * * * * * * * *

P51531|SMC    272 P-STPQKLPVPAPGGRPSAPPAAAQPAAAVPGPSVPQFAPGQPSVQLQOQKQSRISP
P51532|SMC    295 PTSTPQKLIPPQPTGRPSAPPAPVPAASVMPPPQTSFGQPAQPAPMVPLHQKQSRITP
      * ***** * * ***** * * * * * * * * * * * * * * * * * * * *

P51531|SMC    331 IQKPQGLDPVEILQEREYRLQARIAHRIQELENLPGSLPPDLRTKATVELKALRLLNFQR
P51532|SMC    355 IQKPRGLDPVEILQEREYRLQARIAHRIQELENLPGSLAGDLRTKATIELKALRLLNFQR
      **** ***** ***** ***** ***** ***** ***** ***** *****

P51531|SMC    391 QLRQEVVACMRRDTTLETALNSKAYKRSKRQTLREARMTEKLEKQKQIEQERKRRQKHQE
P51532|SMC    415 QLRQEVVVCMRRDTALETALNAKAYKRSKRQSLREARITEKLEKQKQIEQERKRRQKHQE
      ***** ***** ***** ***** ***** ***** ***** ***** *****

P51531|SMC    451 YLNSILQHAKDFKEYHRSVAGKIQKLSKAVATWHANTEREQKKETERIEKERMRLMAED
P51532|SMC    475 YLNSILQHAKDFKEYHRSVTGKIQLTKAVATYHANTEREQKKENERIEKERMRLMAED
      ***** ***** ***** ***** ***** ***** ***** ***** *****

P51531|SMC    511 EEGYRKLIDQKKDRRLAYLLQQTDEYVANLTNLVWEHKQAQAAKEKKRRRRKKKAEENA
P51532|SMC    535 EEGYRKLIDQKKDRRLAYLLQQTDEYVANLTELVRQHAAQVAKEKKKKK--KKKKAENA
      ***** ***** ***** * * * * * * * * * * * * * * * * * * * *

P51531|SMC    571 EGGESALGPDGEPIDESSQMSDLPVKVTHTETGKVLFGPEAPKASQLDAWLEMNPGYEVA
P51532|SMC    593 EGQTPAIGPDGEPLETSQMSDLPVKVIHVESGKILTGTDAPKAGQLEAWLEMNPGYEVA
      **   * ***** * * ***** * * * * * * * * * * * * * * * * * * * *

P51531|SMC    631 PRSDSEESDSYEEEEEDEESSRQET-----EEKILLDPNSEEVSEKDAKQI IETAKQ
P51532|SMC    653 PRSDSEESGSEEEEEEEEEQPQAAQPPTLPVEEKKKIPDPDSDDVSEVDARHI IENAKQ
      ***** *   ** * * * * * * * * * * * * * * * * * * * * * * * * *

P51531|SMC    684 DVDDEYSM-QYSARGSQSYTVAHAISERVEKQSALLINGTLKHYQLQGLEWVSLYNNN
P51532|SMC    713 DVDDEYGVSQLARGLQSYAVAHAVTERVVDKQSALMVNGVLKQYQIKGLEWLVSLYNNN
      ***** *   ** * * * * * * * * * * * * * * * * * * * * * * * * *

P51531|SMC    743 LNGILADEMGLGKTIQTIALITYLMEHKRLNGPYLIIVPLSTLSNWTYEFDKWAPSVVKI
P51532|SMC    773 LNGILADEMGLGKTIQTIALITYLMEHKRINGPFLIIVPLSTLSNWAYEFDKWAPSVVKV
      ***** ***** ***** ***** ***** ***** ***** ***** *****

P51531|SMC    803 SYKGT PAMRRSLVPQLRSGKFNVL LTTYEYI IKDKHILAKIRWKYMI VDEGHRMKNHHCK
P51532|SMC    833 SYKGS PAARRAFV PQLRSGKFNVL LTTYEYI IKDKHILAKIRWKYMI VDEGHRMKNHHCK
      **** * * * * * * * * * * * * * * * * * * * * * * * * * * * * * *

P51531|SMC    863 LTQVLNTHYVAPRRLLTGTPLQNKLP ELWALLN FLLPTIFKSCSTFEQWFNAPFAMTGE
P51532|SMC    893 LTQVLNTHYVAPRRLLTGTPLQNKLP ELWALLN FLLPTIFKSCSTFEQWFNAPFAMTGE
      ***** ***** ***** ***** ***** ***** ***** ***** *****

P51531|SMC    923 RVDLNEEETILII RRLHKVLRPFLLR LKKEVESQLPEKVEYVIKCDMSALQKILYRHMQ
P51532|SMC    953 KVDLNEEETILII RRLHKVLRPFLLR LKKEVEAQLPEKVEYVIKCDMSALQRVLYRHMQ
```

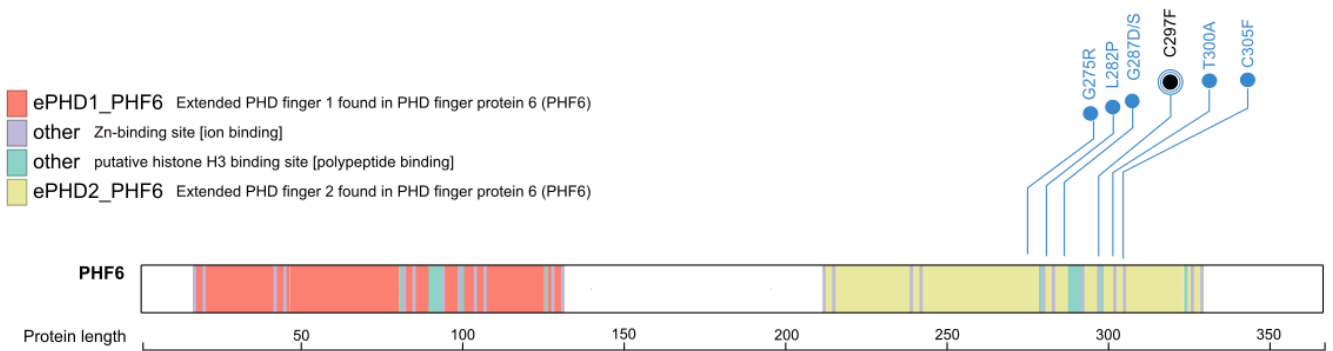
```

*****
P51531|SMC 983 AKGILLTDGSEKDKKGGKAKTLMNTIMQLRKICNHPYMFQHIEESFAEHLGYSNGVING
P51532|SMC 1013 AKGVLLTDGSEKDKKGGTKTLMNTIMQLRKICNHPYMFQHIEESFSEHLGFTGGIVQG
*** ***** * *
P51531|SMC 1043 AELYRASGKFELLDRIPLKLRATNHRVLLFCQMTSLMTIMEDYFAFRNFLYLRLDGTGTS
P51532|SMC 1073 LDLYRASGKFELLDRIPLKLRATNHKVVLLFCQMTSLMTIMEDYFAYRGFKYLRLDGTGTTKA
***** * * *****
P51531|SMC 1103 EDRAALLKKFNPEGSQYFIFLLSTRAGGLGGLNLQAADTVVIFDSDWNPHQDLQAQDRAHR
P51532|SMC 1133 EDRGMLLKTFFNEPGSEYFIFLLSTRAGGLGGLNLQSADTVIIFDSDWNPHQDLQAQDRAHR
*** * * ***** * * *****
P51531|SMC 1163 IGQQNEVRVLRRLCTVNSVVEEKILAAAKYKLNVDQKVIQAGMFDQKSSSHERRAFLQAILE
P51532|SMC 1193 IGQQNEVRVLRRLCTVNSVVEEKILAAAKYKLNVDQKVIQAGMFDQKSSSHERRAFLQAILE
*****
P51531|SMC 1223 HEEENE-----EEDEVDPDETTLNQMIAARREEE
P51532|SMC 1253 HEEQDES RHCSTGSGSASFHTAPPAGVNPDLLEPPLKEEDEVDPDETTLNQMIAARHEEE
*** * ***** * * *
P51531|SMC 1250 FDLFMRMDRRREDARNPKRKPRLMEEDELPSWIIKDDAEVERLTCEEEEEKIFGRGSR
P51532|SMC 1313 FDLFMRMDLDRREEARNPKRKPRLMEEDELPSWIIKDDAEVERLTCEEEEEKMFGRGSR
***** * * *****
P51531|SMC 1310 QRRVDVYSDALTEKQWLRAIEDGNLEEMEEVRLKRRRRNVKDPDPA-----
P51532|SMC 1373 HRKEVDYSDSLTEKQWLKAIEEGTLEEIEEEVVRQKKSRRKRKRDSDAGSSTPTTSTRSRD
* * * * * * * * * * * * * * * *
P51531|SMC 1358 KEDVEKAKRRRGRPPAEKLSNPNNPKLTKQMNAIIDTVINYKDRCNVEKVPNSQLEIEGN
P51532|SMC 1433 KDDESKKQKRRGRPPAEKLSNPNNLTKMKKIIVDAVIKYKD-----S
* * * * * * * * * * * * * * * *
P51531|SMC 1418 SSGRQLSEVFIQLPSRKELPEYYELIRKPVDFKKIKERIRNHKYRSLGDLEKDVMLLCHN
P51532|SMC 1476 SSGRQLSEVFIQLPSRKELPEYYELIRKPVDFKKIKERIRNHKYRSLNDLEKDVMLLQCN
***** *
P51531|SMC 1478 AQTFNLEGSQIYEDSIVLQSVFKSARQKIAKEEESSEDESNEEEEEDEEESSESEAKSVKV
P51532|SMC 1536 AQTFNLEGS LIYEDSIVLQSVFTSVRQKIEKEDDSEGESEEEEEEGEESSESRSVKV
***** * * * * * * * * * *
P51531|SMC 1538 KIKLNKDDKGRDKGKGRPNRG-KAKPVVSDFDSDEEQDEREQSEGS GTD
P51532|SMC 1596 KIKLGRKEKAQDRLLKGGRRRPSRGSRAKPVVSDDDSEEEQEEDRS GSGSEED
*** * * * * * * * * * * * * * *

```

Supplemental figure S2: Multiple sequence alignment (MSA) between human SMARCA2 and SMARCA4 proteins.

Sequence alignment between human SMARCA2 (P51531) and SMARCA4 (P51532) proteins by SIM - Alignment Tool for Protein Sequences (<https://web.expasy.org/sim/>) using preset parameters. The alignment shows a 73.9% identity in 1672 residues overlap.



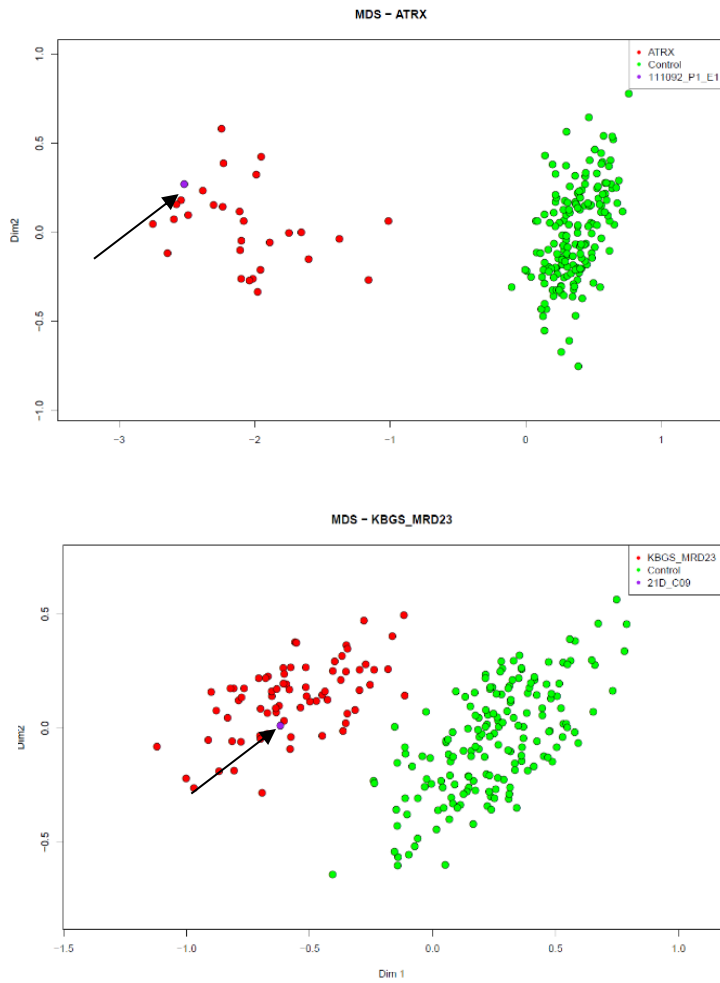
Supplemental figure S3: Reported missense variants in *PHF6* affected females.

Schematic drawing of literature reported missense variants in *PHF6* gene (NM_001015877)¹³, using PeCan, St. Jude Cloud (<https://pecan.stjude.cloud>) software.



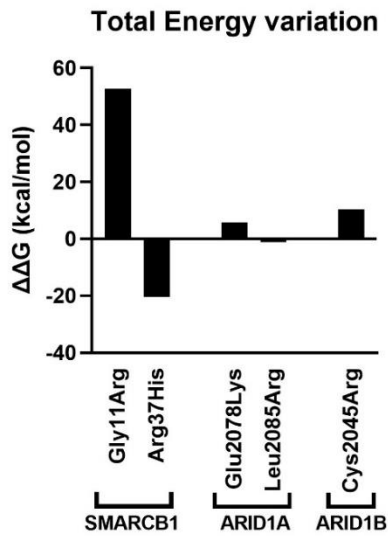
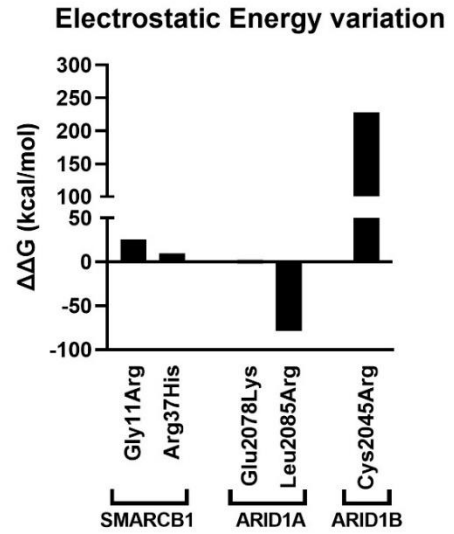
Supplemental figure S4: Impact on splicing of the NM_153252.5: c.1233-7_1233-3 variant in *BRWD3*

The impact of the NM_153252.5: c.1233-7_1233-3 variant in *BRWD3* was computed using AlamutVisualPlus software (ver1.7.1). The change is likely to affect the acceptor splice site of exon 14/41 as predicted by at least three softwares (MaxEnt: -79.8%; NNSPLICE: -99.4%; SSF: -19.2%; overall -66.1%). The consequence of this change on the mRNA is however to be tested experimentally on cDNA from the patient.



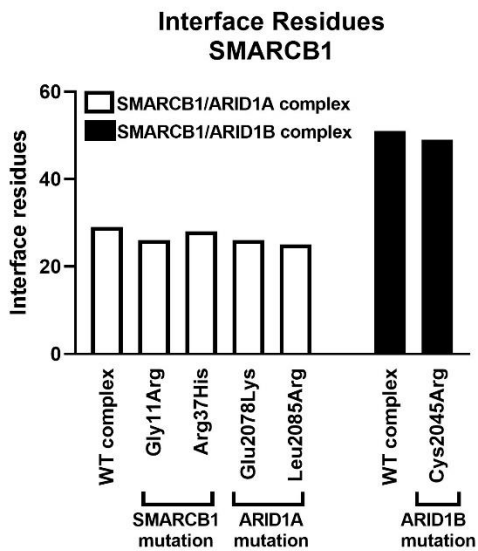
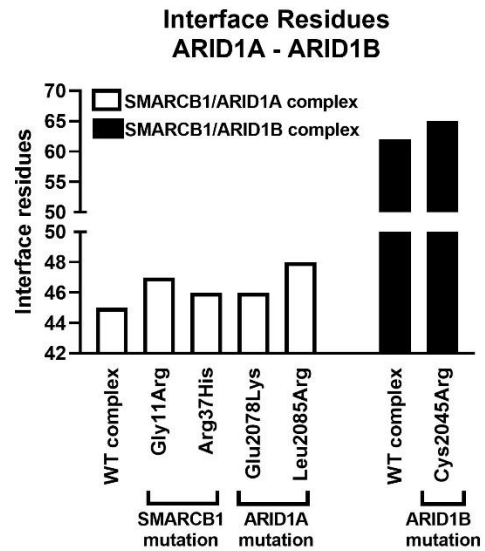
Supplemental figure S5: MDS plots for ATRX and KBG & MRD23 episignature profiling

Multidimensional scaling (MDS) plots: upper panel- ATRX gene (MIM# 301040); green: controls, red : cases, purple: case 111092, lower panel- ANKRD11 (KBG MIM#148050) & SETD5 (MRD23 MIM #615761); green :controls, red :cases, purple: case NWM-021D.

A**B**

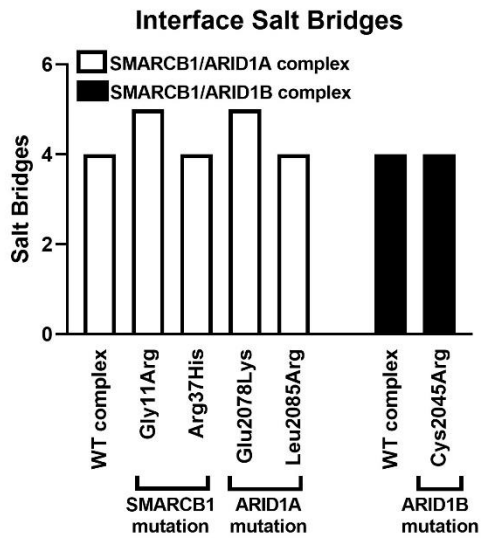
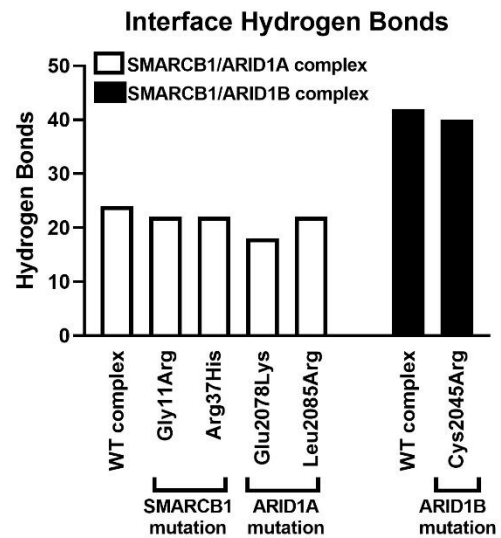
Supplemental figure S6 Energies calculated on the PDB complex (based on PDB id 6LTH)

Energy variation upon mutation and minimization (mutant-WT) estimated with the forcefield AMBER 12: EHT. Brackets below indicate which protein is the mutant product in the complex. A) is the sum of all energy terms, B) considers just the electrostatic term.

A**B**

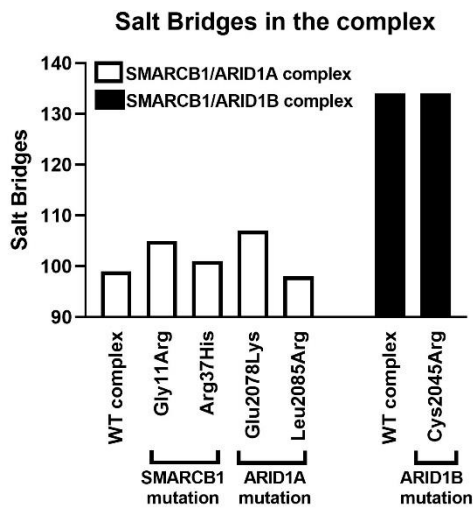
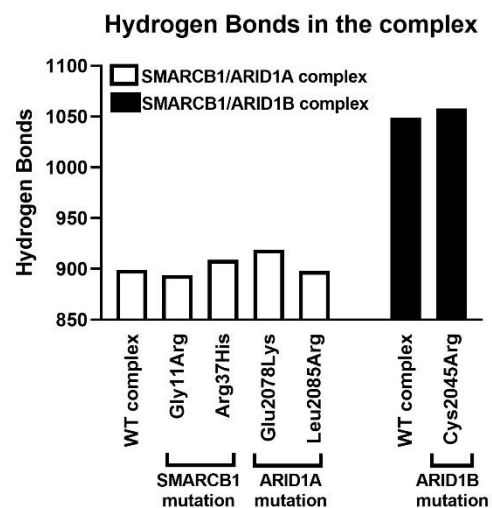
Supplemental figure S7: Residues at the complex interface (based on PDB id 6LTH)

Number of residues present at the interface between the proteins (SMARCB1/ARID1A, and SMARCB1/ARID1B complex). A) SMARCB1 residues, B) ARID1A/ARID1B residues.

A**B**

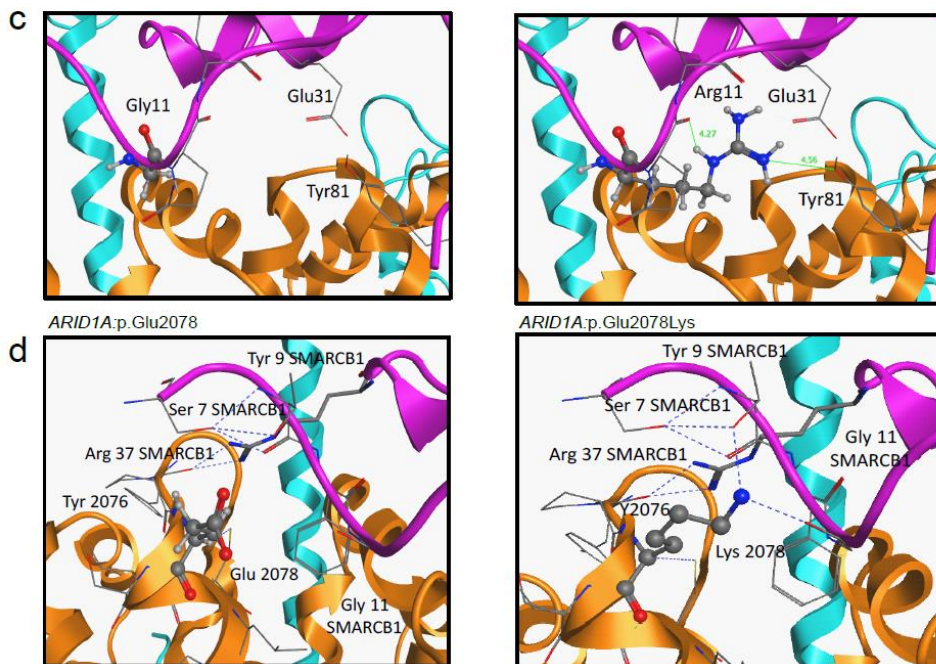
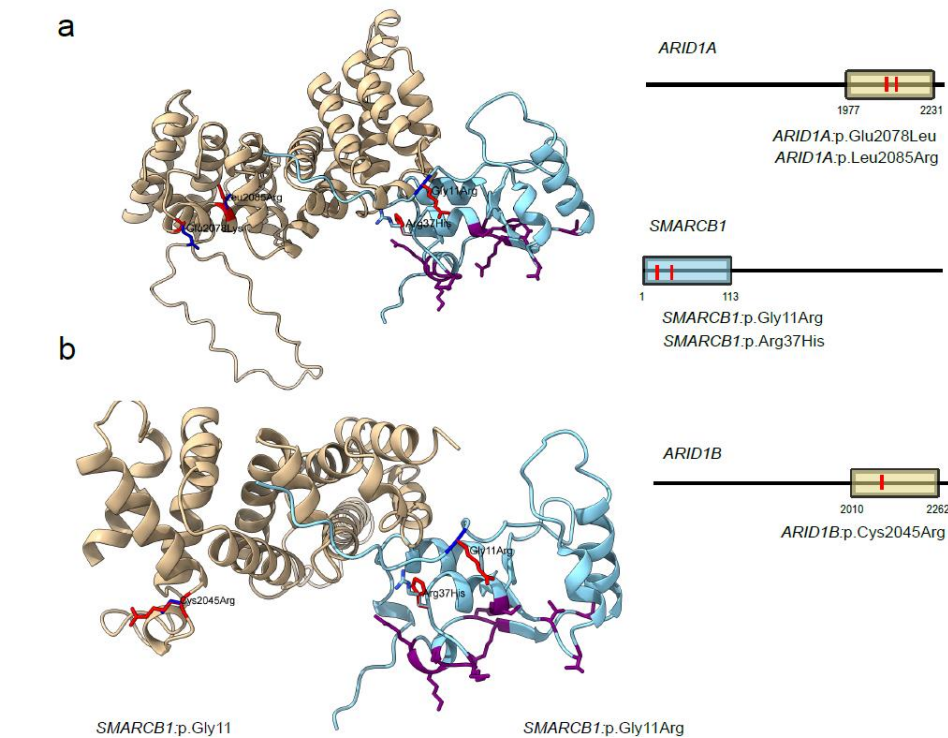
Supplemental figure S8: Interactions at the complex interface (based on PDB id 6LTH)

Number of Salt Bridges (A), and Hydrogen Bonds (B) at the interface between the proteins (SMARCB1/ARID1A, and SMARCB1/ARID1B complex).

A**B**

Supplemental figure S9: total interactions in the complex (based on PDB id 6LTH)

Total number of Salt Bridges (A), and Hydrogen Bonds (B) in the whole complex.



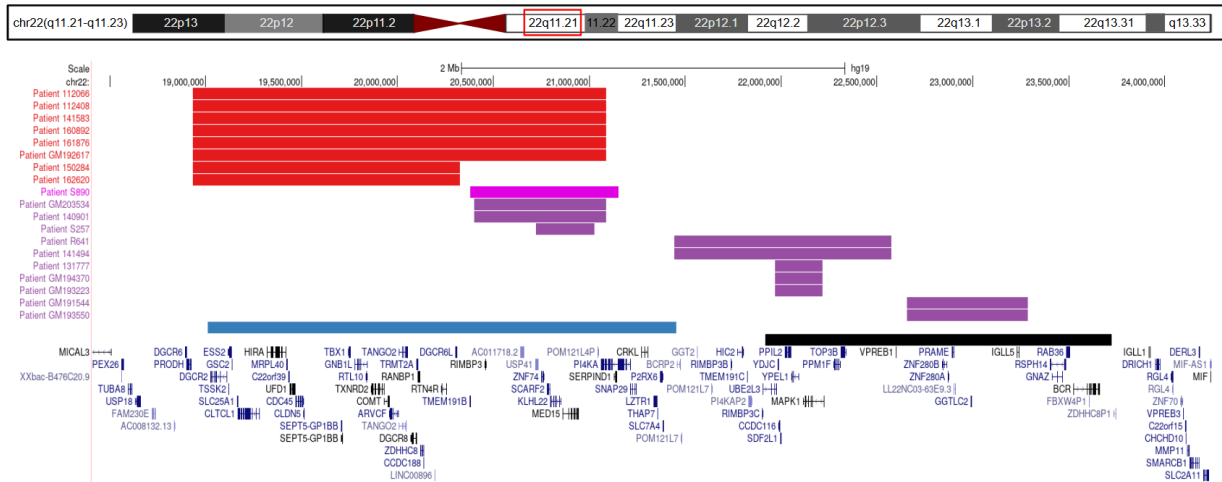
Supplemental figure S10. Comparison of ARID1A/ARID1B paralogues and SMARCB1 interacting amino acids.

Panel a: ARID1A-yellow-DUF3518 domain (a.a 1977-2231) SMARCB1-blue-DNA -binding domain (a.a 1-113) red:variant blue:wt purple:codons from DNA -binding domain of SMARCB1 that are in contact with DNA. **Panel b:** ARID1B-yellow-BAF250_C domain(a.a 2010-2262) red:variant blue:wt purple:codons from DNA -binding domain of SMARCB1 that are in contact with DNA;¹⁴ (ARID1A- AlphaFold model:AF-O14497-F1, SMARCB1-AlphaFold model:F-Q12824-F1; ARID1B- AlphaFold model:AF-Q8NFD5-F1; modeled with UCSF ChimeraX version: 1.4 (www.cgl.ucsf.edu/chimerax) using the rotamers-tools function.

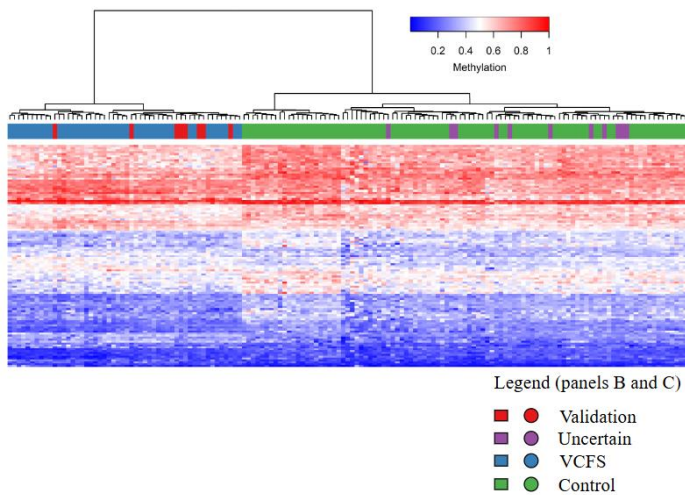
C) Representative caption of the comparison between the sidechains of Gly11 SMARCB1 (WT), and Arg11

(Mutant) revealing the mutant residue involved in newly formed interactions. D) Caption of mutant p.(D2078K) SMARCB1 showing that the side chain of the mutant residue is inserted in an interaction (HB) network.

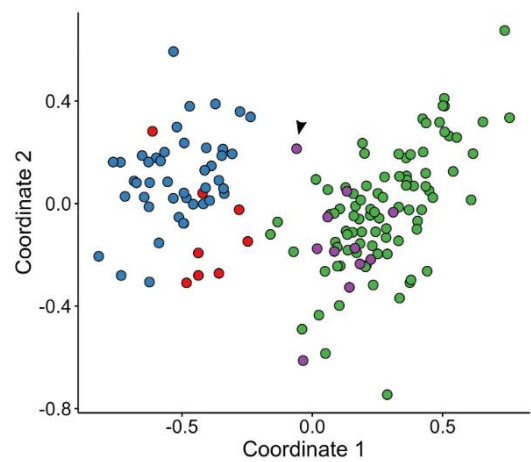
A



B



C



Supplemental figure S11. Episignature analysis of CNVs in the 22q11.2 region.

A. Scheme of the 21 CNVs at 22q11.2 region reported in Table 1 (Validation cohort).

B, C. heatmap and MDS plot show that only the typical 22q11.2DS shows the associated Episignature profiles. Case S890 is clustering nearby 22q11.2DS cases, for unknown reasons (black arrow).

Supplemental Table 1. List of the cases analysed, ACMG/AMP variant classification and HPO terms

Sample ID	Sex	Phenotyp	Gene/ region involved	Ref Seq	Variant	ACMG/ AMP- criteria	classification/ score	HPO
Validation cohort: Single Nucleotide Variants (SNVs) (34 cases)								
NWM-030D	F	Helsmoortel-van der Aa syndrome	<i>ADNP</i>	NM_001282531.3	c.539_542del:p.(Val180fs)	PVS1; PM2;PP5	P	HP:0001252-Muscular hypotonia;HP:0001249-Intellectual disability
GM223306	F	Helsmoortel-van der Aa syndrome	<i>ADNP</i>	NM_001282531.3	c.2454C>G:p.(Tyr818Ter)	PVS1; PM2;PP5	P	HP:0001249-Intellectual disability; HP:0012758-Neurodevelopmental delay
121623	M	KBG syndrome	<i>ANKRD11</i>	NM_013275.6	c.439C>T:p.(Gln147*)	PVS1; PM2;PP5	P	HP:0001510-Growth delay, HP:0001156-Brachydactyly, HP:0000824-Decreased response to growth hormone stimulation test , HP:0011342-Mild global developmental delay, HP:0001629-Ventricular septal defect , HP:0000271-Abnormality of the face
BA2012002	F	KBG syndrome	<i>ANKRD11</i>	NM_013275.6	c.211_226+1del	PVS1; PM2;PP5	P	HP:0001249-Intellectual disability;HP:0011342-Mild global developmental delay,
NWM-218D	M	KBG syndrome	<i>ANKRD11</i>	NM_013275.6	c.1903_1907del:p.Lys635fs	PS4;PVS1; PM2;PP5	P	HP:0001249-Intellectual disability; HP:0001250-Seizures;HP:0001344-Absent speech;HP:0001290-Generalized hypotonia
NMW-035D	M	Coffin-Siris syndrome 2	<i>ARID1A</i>	NM_006015.6	c.6232G>A:p.(Glu2078Lys)	PS2;PM2;PP2;PP3	LP	HP:0001249; HP:0001655; HP:0001642;HP:0007376;HP:0002804;HP:00010311; HP:00028;HP:0001845;HP:00023;HP:0001290;HP:000767;HP:00030215;HP:000954;HP:000396;HP:000347;HP:000280; HP:000316;HP:000286; HP:00012810; HP:0002714;HP:000470;HP:000369;HP:00012385;HP:000474;HP:000582;HP:0006191;
160759	F	Coffin-Siris syndrome 1	<i>ARID1B</i>	NM_001374828.1	c.5825G>A:p.(Trp1942*)	PVS1; PS2; PM2	LP	HP:0001249-Intellectual disability;
142220	M	CHARGE syndrome	<i>CHD7</i>	NM_017780	c.3082A>G:p.(Ile1028Val)	PM1;PM2; PP2;PP3; PP5	LP	HP:0001249-Intellectual disability; HP:0008501-Median cleft lip and palate
FS0208013	M	CHARGE syndrome	<i>CHD7</i>	NM_017780	c.6194G>A:p.(Arg2065His)	PM1;PM2; PP2;PP3; PP5	LP	HP:0001249-Intellectual disability;
GM110562	M	Autism, susceptibility to	<i>CHD8</i>	NM_001170629.2	c.2025-1G>C	PVS1; PS2; PM2;PP5	LP	HP:0001249-Intellectual disability; HP:0001548-Overgrowth; HP:0000316-Hypertelorism; HP:0005280-Depressed nasal bridge; HP:0000286-Epicanthus; HP:0001263-Global developmental delay
110212	M	Rubinstein-Taybi syndrome 1	<i>CREBBP</i>	NM_004380.3	c.3779+1G>A	PVS1; PS2; PM2;PP5	P	HP:0001680-Coarctation of aorta; HP:0001647-Bicuspid aortic valve ; HP:0001633-Abnormal mitral valve morphology; HP:0001507-Growth abnormality;

141444	M	Kleefstra syndrome 1	<i>EHMT1</i>	NM_02475 7.5	c.3331T>A:p.(Cys111Ser)	PS1;PS2;PM2;PP3	P	HP:0000729-Autistic behavior , HP:0006335-Persistence of primary teeth , HP:0000023-Inguinal hernia , HP:0000646-Amblyopia , HP:0001763- Pes planus , HP:0001263-Global developmental delay , HP:0000750, Stereotypy HP:0000733-Delayed speech and language development, HP:0001388-Joint laxity , HP:0000767-Pectus excavatum , HP:0007018-Attention deficit hyperactivity disorder, HP:0007057-Poor hand-eye coordination, HP:0000272-Malar flattening , HP:0000676-Abnormality of the incisor
131361	M	Kleefstra syndrome 1	<i>EHMT1</i>	NM_02475 7.5	c.3000del:p.(Asp1001fs)	PVS1; PS2; PM2;PP5	P	HP:0001643- Patent ductus arteriosus, HP:0001249- Intellectual disability; HP:0002870-Obstructive sleep apnea
GM181933	M	Kleefstra syndrome	<i>EHMT1</i>	NM_02475 7.5	c.508del:p.(Gln170fs)	PVS1; PS2; PM2;PP5	P	HP:0001263-Global developmental delay;HP:0001256-Intellectual disability,
GM184039	F	Rubinstein-Taybi syndrome 2	<i>EP300</i>	NM_00142 9.4	c.3671+5G>C	PS2; PS3;PM2;PM4;P3	LP	HP:0001511-Intrauterine growth retardation; HP:0001561-Polyhydramnios , HP:0001518-Small for gestational age, HP:0011451-Primary microcephaly, HP:0001669-Transposition of the great arteries, , HP:0000365-Hearing impairment , HP:0001510-Growth delay, HP:0001263-Global developmental delay, HP:0000664-Synophrys , HP:0002553-Highly arched eyebrow, HP:0000470-Short neck, HP:0010711-1-2 toe syndactyly , HP:0025419-Pulmonary pneumatocele, HP:0005403-T lymphocytopenia
NWM-019D	M	Weaver syndrome	<i>EZH2</i>	NM_00445 6.5	c.2015T>G:p.(Phe672Cys)	PS2;PM1;PM2;P2;PP3	LP	HP:0001249;HP:0008935;HP:0002721;HP:0001537;HP:000028;HP:0003037;HP:0005616;HP:0001655;HP:0004684;HP:000100806;HP:0004324;HP:000280;HP:000311;HP:0008070;HP:000256;HP:00011220;HP:0005469;HP:0001090;HP:000316;HP:000369;HP:0005280;HP:000343;HP:000218;HP:000277;HP:000470;HP:0001812;HP:00012385;HP:00030084;HP:0009381;HP:00010300 ;
NWM-088D	F	Rahman syndrome	<i>HIST1H1E</i>	NM_00532 1.3	c.458_460del:p.(Lys152fs)	PVS1; PM2;PP3	P	HP:0001263; HP:000717; HP:0002691; HP:00040194; HP:000280; HP:000337;HP:000490;HP:0007874;HP:000316;HP:000431; HP:000322; HP:0009765;HP:000455;HP:000303;HP:00040170;HP:0001182; HP:0007565;HP:000670;HP:000958;HP:000207;HP:0008070;
GM201880	F	Mental retardation, autosomal dominant 32	<i>KAT6A</i>	NM_00676 6.5	c.2927del:p.(Gly976Valfs)	PVS1;PS2; PM2	P	HP:0001263-Global developmental delay;HP:0001256-Intellectual disability,

121116	M	Intellectual developmental disorder, X-linked, Claes-Jensen type	<i>KDM5C</i>	NM_004187.5	c.1204G>A:p.(Asp402Asn)	PM2;PM5;PP2;PP5	LP	HP:0001249-Intellectual disability, HP:0000750-Delayed speech and language development;
121886	F	Intellectual developmental disorder, X-linked, Claes-Jensen type	<i>KDM5C</i>	NM_004187.5	c.1204G>A:p.(Asp402Asn)	PM2;PM5;PP2;PP5	LP	HP:0011342-Mild global developmental delay
121888	F	Intellectual developmental disorder, X-linked, Claes-Jensen type	<i>KDM5C</i>	NM_004187.5	c.1204G>A.(Asp402Asn)	PM2;PM5;PP2;PP5	LP	not affected
NWM-192D	F	WDSTS	<i>KMT2A</i>	NM_001197104.2	c.4777del:p.(Arg1593fs)	PVS1;PS2;PM2;PP5	P	HP:0001249-Intellectual disability, HP:0001518-Small for gestational age;HP:0000824-Growth hormone deficiency;HP:0000826-Precocious puberty;
GM194228	M	Kabuki syndrome 1	<i>KMT2D</i>	NM_003482.3	c.4395dup:p.(Lys1466fs)	PVS1,PM2,PP5	P	HP:0001249-Intellectual disability,
NWM-031D	F	Kabuki	<i>KMT2D</i>	NM_003482.3	c.13795_13802del:p.(Ala4599fs)	PVS1;PS2;PM2;PP3	P	HP:0001249;HP:0001319;HP:000343;HP:000337;HP:000316;HP:00012810;HP:000637;HP:0002553;HP:00011229;HP:000358;HP:0001212;HP:00010314
NWM-024D	F	Börjeson-Forssman-Lehmann syndrome	<i>PHF6</i>	NM_001015877.2	c.890G>T:p.(Cys297Phe)	PS2;PM1;PM2;PP2;PP3	LP	HP:0001263;HP:000717;HP:000175;HP:0001537;HP:0001290;HP:0001643;HP:0001156;HP:0004691;HP:000280;HP:000486;HP:000574;HP:000316;HP:000506;HP:000582;HP:000343;278;HP:000369;HP:000470;HP:000664;HP:00011229
NWM-163D1	M	Renpenning syndrome	<i>PQBPI</i>	NM_001032383.2	c.457_459del:p.(Arg153fs)	PVS1;PM2;PP3	P	HP:0001249-Intellectual disability,HP:0002194-Delayed gross motor development
NWM-163D2	M	Renpenning syndrome	<i>PQBPI</i>	NM_001032383.2	c.457_459del:p.(Arg153fs)	PVS1;PM2;PP3	P	HP:0001249-Intellectual disability,HP:0002194-Delayed gross motor development
GM182051	M	Renpenning syndrome	<i>PQBPI</i>	NM_001032383.2	c.233C>A:p.(Pro78Gln)	PM1;PM2;PM5;PP2;PP3;	LP	HP:0001250; HP:0010864; HP:0002415; HP:0001510; HP:0000118
GM173348	F	SETD1B-related syndrome	<i>SETD1B</i>	NM_001353345.2	c.598del:p.(Gln200fs)	PVS1;PS1;PS2;PM2;PP3	P	HP:0002342-Intellectual disability, moderate, HP:0012420-Meconium stained amniotic fluid, HP:0000750-Delayed speech and language development, HP:0001081-Cholelithiasis
GM223349	M	Intellectual developmental disorder,	<i>SETD5</i>	NM_001080517.3	c.868_872del:p.(Arg290fs)	PVS1;PS2;PM2	P	HP:0001249-Intellectual disability; HP:0001999-Abnormal facial shape, HP:0000047-Hypospadias, HP:0000028-Cryptorchidism

		autosomal dominant 23						
GM223350	F	Intellectual developmental disorder, autosomal dominant 23	<i>SETD5</i>	NM_001080517.3	c.3848_3849insC:p.(Ser1286fs)	PVS1;PS2;PM2	P	HP:0001572-Macrodonia; HP:0001249-Intellectual disability; HP:0004322-Short stature; HP:0000924-Abnormality of the skeletal system; HP:0001999-Abnormal facial shape
GM190941	M	Coffin-Siris syndrome 4	<i>SMARCA4</i>	NM_003072.5	c.3068A>G:p.(Glu1023Gly)	PS2;PM2;PP2;PP3	LP	HP:0006889-Intellectual disability, borderline, HP:0011968-Feeding difficulties, HP:0000708-Behavioral abnormality, HP:0000736-Short attention span, HP:0000750-Delayed speech and language development, HP:0002353-EEG abnormality, HP:0025313-Exophoria, HP:0100702-Arachnoid cyst;HP:0011937-Hypoplastic fifth toenail, HP:0010935-Abnormality of the upper urinary tract, HP:0000768- Pectus carinatum
GM223379	F	Coffin-Siris syndrome 4	<i>SMARCA4</i>	NM_003072.5	c.1646G>T:p.(Arg549Leu)	PS2;PM2;PP2;PP3	LP	HP:0001249-Intellectual disability;
GM223380	F	Coffin-Siris syndrome 3	<i>SMARCB1</i>	NM_003073.5	c.110G>A:p.(Arg37His)	PM2;PP2;PP3;PP5	LP	HP:0001249-Intellectual disability, HP:0000238-Hydrocephalus, HP:0002273-Tetraparesis, HP:0002247-Duodenal atresia, HP:0000518-Cataract
GM183514	F	Cornelia de Lange syndrome 2	<i>SMC1A</i>	NM_006306.4	c.1276_1282del:p.(Arg426fs)	PVS1;PS2;PM2;	LP	HP:0001249-Intellectual disability; HP:0001250-Seizures
130091	M	Coffin-Siris syndrome 9	<i>SOX11</i>	NM_003108.3	c.159G>T :p.(Met53Ile)	PS2;PM1;PM2;PP2;PP3	P	Neurodevelopmental delay HP:0012758, Behavioral abnormality HP:0000708, Cleft palate HP:0000175, Absent speech HP:0001344, Inguinal hernia HP:0000023
131749	F	FLHS	<i>SRCAP</i>	NM_006662.3	c.7937_7938del:p.(Val264fs)	PVS1;PS2;PM2;PP5	P	Autistic behavior HP:0000729, Intellectual disability, mild HP:0001256, Delayed speech and language development HP:0000750, Self-injurious behavior HP:0100716, Growth delay HP:0001510, Abnormal facial shape HP:0001999
Validation cohort: Copy Number Variants (CNVs) (25 cases)								
NWM-020D	F	Mental retardation, autosomal dominant 23	<i>SETD5</i>	GRCh[38]-CNV loss	3p25.3(9091710-12334937)x1	L1A;L2A;L3C;L4E;L5F	P-2.00	HP:00001249; HP:00001252; HP:000010767;HP:00001643;HP:000040253;HP:00001162; HP:00001159;HP:000011231;HP:000011333;HP:0000337;HP:0000490;HP:0000506;HP:0000431;HP:0000368;HP:0000396;HP:0000395;HP:0000343;HP:0000325;HP:0000276;HP:0000331;HP:000010211;HP:0000494
162391	M	Mental retardation, autosomal dominant 23	<i>SETD5</i>	GRCh[38]-CNV loss	3p26.3(52266-10683525)x1	L1A;L2A;L3C;L4E;L5F	P-2.00	HP:0001249-Intellectual disability

GM190395	F	Wolf-Hirschhorn syndrome	Chr4p16.13 del	GRCh[38]-CNV loss	4p16.13(71660-6479683)x1	L1A;L2A;L3C;L4E;L5F	P-2.0	HP:0001249-Intellectual disability;
GM200157	F	Wolf-Hirschhorn syndrome	Chr4p16.13 del	GRCh[38]-CNV loss	4p16.13(71660-13395123)x1	L1A;L2A;L3C;L4E;L5F	P-2.0	HP:0001249-Intellectual disability;
T223	M	Sotos syndrome	Chr.5q35	GRCh[38]-CNV loss	5q35(176463495-177956831)x1	L1A;L2A;L3C;L4E;L5F	P-2.00	HP:0100543-Cognitive impairment
S288	M	Hunter McAlpine syndrome	Chr.5q35-qter.dup	GRCh[38]-CNV gain	5q35(176412680-177477797)x3	G1A;G2A;G3B;L4B;L5A	P-2.05	HP:0000047-Hypospadias;HP:0003510-Severe short stature;HP:0000252-Microcephaly;HP:0000750-Delayed speech and language development; HP:0001263-Global developmental delay
GM201583	F	Williams-Beuren syndrome	Chr7q11.23 del	GRCh[38]-CNV loss	7q11.23(73312582-74924037)x1	L1A;L2A;L3C;L4E;L5F	P-2.0	HP:0001627-Abnormal heart morphology;
GM192375	M	Suspected Williams-Beuren syndrome	Chr7q11.23 del	GRCh[38]-CNV loss	7q11.23(73312582-74725057)x1	L1A;L2A;L3B;L4J;L5B	VUS-0.85	HP:0001249-Intellectual disability;
GM193789	F	Chr7q11.23 duplication syndrome	Chr7q11.23 dup	GRCh[38]-CNV gain	7q11.23(73312582-74725057)x3	G1A;G2A;G3A;L4E;L5F	P-1.10	HP:0001249-Intellectual disability;
111884	F	Kleefstra syndrome 1	<i>EHMT1</i>	GRCh[38]-CNV loss	9q34.3(136428708-138059695)x1	L1A;L2A;L3C;L4E;L5F	P-2.00	HP:0005176-Dysplastic aortic valve;HP:0000316-Hypertelorism;HP:0010804-Tented upper lip vermillion; HP:0000179-Thick lower lip vermillion; HP:0001290-Generalized hypotonia; HP:0011451-Primary microcephaly;HP:0001263-Global developmental delay;HP:0001250-Seizure
131568	F	Kleefstra syndrome 1	<i>EHMT1</i>	GRCh[38]-CNV loss	9q34.3(137447506-137984409)x1	L1A;L2A;L3A;L4E;L5F	P-1.10	HP:0100543-Cognitive impairment;HP:0001249-Intellectual disability;
161978	M	Kleefstra syndrome	<i>EHMT1</i>	GRCh[38]-CNV loss	9q34.3(135866376-138114463)x1	L1A;L2A;L3C;L4E;L5F	P-2.00	HP:0001999-Abnormal facial shape;HP:0001249-Intellectual disability
GM181473	F	Kleefstra syndrome 1	<i>EHMT1</i>	GRCh[38]-CNV loss	9q34.3(137666340-138059695)x1	L1A;L2A;L3A;L4E;L5F	P-1.10	HP:0001249-Intellectual disability;HP:0001007-Hirsutism
N821	F	Suspected Rubinstein Taybi	<i>CREBBP</i>	GRCh[38]-CNV loss	16p13.3(3461539-3805666)x1	L1A;L2C-1;L3A;L4E;L5F	P-1.00	
112066	M	Velocardiofacial syndrome	Chr.22q11.21del	GRCh[38]-CNV loss	22q11.21(18932429-21086225)x1	L1A;L2A;L3C;L4A;L5H	P-2.35	HP:0100543-Cognitive impairment
112408	M	Velocardiofacial syndrome	Chr.22q11.21del	GRCh[38]-CNV loss	22q11.21(18932429-21086225)x1	L1A;L2A;L3C;L4A;L5H	P- 2.35	HP:0100702-Arachnoid cyst; HP:0000750-Delayed speech and language development;HP:0001263-Global developmental delay
141583	M	Velocardiofacial syndrome	Chr.22q11.21del	GRCh[38]-CNV loss	22q11.21(18932429-21086225)x1	L1A;L2A;L3C;L4A;L5H	P- 2.35	HP:0001249-Intellectual disability;
160892	M	Velocardiofacial syndrome	Chr.22q11.21del	GRCh[38]-CNV loss	22q11.21(18932429-21086225)x1	L1A;L2A;L3C;L4A;L5H	P- 2.35	HP:0002463-Language impairment

161876	F	Velocardiofacial syndrome	Chr.22q11.21del	GRCh[38]-CNV loss	22q11.21(18932429-21086225)x1	L1A;L2A;L3C;L4A;L5H	P- 2.35	HP:0001249-Intellectual disability; HP:0005684-Distal arthrogryposis;
GM192617	F	Velocardiofacial syndrome	Chr.22q11.21del	GRCh[38]-CNV loss	22q11.21(18932429-21086225)x1	L1A;L2A;L3C;L4K;L4M;L5E	P-1.75	HP:0001249-Intellectual disability;HP:0001250
150284	M	Velocardiofacial syndrome	Chr.22q11.21del	GRCh[38]-CNV loss	22q11.21(18932429-20324240)x1	L1A;L2A;L3C;L4E;L5H	P-2.15	HP:0001249-Intellectual disability;HP:0100753-Schizophrenia
162620	M	Velocardiofacial syndrome	Chr.22q11.21del	GRCh[38]-CNV loss	22q11.21(18932429-20324240)x1	L1A;L2A;L3C;L4E;L5H	P-2.15	HP:0001249-Intellectual disability; HP:0001611-Nasal speech
142071	F	Koolen de Vreys syndrome	<i>KANSL1</i>	GRCh[38]-CNV loss	17q21.3(45640337-46082496)x1	L1A;L2A;L3A;L4C;L5A	P-1.55	HP:0001263-Global developmental delay
152118	F	Koolen de Vreys syndrome	<i>KANSL1</i>	GRCh[38]-CNV loss	17q21.3(45640337-46133456)x1	L1A;L2A;L3A;L4C;L5A	P-1.55	HP:0001680-Coarctation of aorta; HP:0001629-Ventricular septal defect;HP:0001249-Intellectual disability
GM181681	F	Koolen de Vreys syndrome	<i>KANSL1</i>	GRCh[38]-CNV loss	17q21.3(45640337-46267672)x1	L1A;L2A;L3A;L4E;L5F	P-1.1	HP:0001249-Intellectual disability;HP:0001274-Agenesis of corpus callosum
Validation of SNV/CNV VUS /no variant (18 cases)								
160708	M	Coffin-Siris syndrome 1	<i>ARID1B</i>	NM_001374828.1	c.2480C>T:p.(Ala827Val)	PM2;PP5	VUS	HP:0000729-Autistic behavior, HP:0012758-Neurodevelopmental delay , HP:0001250-Seizure , HP:0000126-Hydronephrosis, HP:0012741-Unilateral cryptorchidism, HP:0012646-Retractile testis
150163	M	Coffin-Siris syndrome 1	<i>ARID1B</i>	NM_001374828.1	c.3589G>A:p.(Asp1197Asn)	PP5	VUS	HP:0000729-Autistic behavior, HP:0001263-Global developmental delay, HP:0000664-Synophrys (mild), HP:0031770 (mild)-Epicanthus palpebralis , HP:0000233-Thin vermilion border , HP:0000343-Long philtrum, HP:0000319-Smooth philtrum, HP:0000430-Underdeveloped nasal alae, HP:0000193-Bifid uvula
NWM-116D	M	Mental retardation, XL 93	<i>BRWD3</i>	NM_153252.5	c.1233-7_1233-3del	PM2;	VUS	HP:0001249-Intellectual disability;
GM173400	F	Nicolaides-Baraitser syndrome	<i>SMARCA2</i>	NM_003070.5	c.2566A>G,p.(Met856Val)	PM2;PP2;PP3	VUS	HP:0001264-Spastic diplegia;HP:0000483-Astigmatism;HP:0002714-HP:0002003-Large forehead; Downturned corners of mouth;HP:0000316-Hypertelorism;HP:0001182-Tapered fingers;HP:0004209-Clonodactyly of the 5th finger
GM203135	F	Phenotype not corresponding to Wiedemann-Steinert	<i>KMT2A</i>	NM_001197104.2	c.5959G>A:p.(Glu1987Lys)	PM2;PP2;PP3	VUS	HP:0004313; HP:0030991; HP:0000776; HP:0000252; HP:0006872
140556	M	Nicolaides-Baraitser syndrome	<i>SMARCA2</i>	NM_003070.5	c.2296C>G:p.(Leu766Val)	PM1;PM2;PP2;PP3	VUS	HP:0009800-Maternal diabetes , HP:0006889-Intellectual disability, borderline, HP:0001328-Specific learning disability , HP:0010522-Dyslexia , HP:0025499-Class I obesity.

140558	M	Nicolaide s- Baraitser syndrome	<i>SMARCA2</i>	NM_003070.5	c.2296C>G:p.(Leu766Val)	PM1; PM2; PP2; PP3	VUS	HP:0006889-Intellectual disability, borderline, HP:0001511:Intrauterine growth retardation , HP:0000750:Delayed speech and language development , HP:0007018:Attention deficit hyperactivity disorder, HP:0000708 :Behavioral abnormality, HP:0001741:Phimosis , HP:0010535 Sleep apnea
NWM-236D	F	Cornelia de lange-like phenotype	<i>NIPBL</i>	?	?	?	?	HP:0001249-Intellectual disability, HP:0000002-Abnormality of body height;HP:0001518-Small for gestational age;HP:0001622-Premature birth;HP:0001655-Patent foramen ovale;HP:0000664-Synophrys;HP:0000347-Micrognathia
S890	M	Velocardiofacial syndrome	Chr.22q11.21del	GRCh[38]-CNV loss	22q11.21(20379137-21151128)x1	L1A;L2A;L3C;L4C;L5A	P-2.45	HP:0001629-Ventricular septal defect;HP:0001363-Craniosynostosis;HP:0000176-Submucous cleft hard palate; HP:0003414-Atlantoaxial dislocation; HP:0008440-C1-C2 vertebral abnormality; HP:0002308-Chiari malformation; HP:0001263-Global developmental delay; HP:0003396-Syngomyelia
GM203534	F	Velocardiofacial syndrome	Chr.22q11.21del	GRCh[38]-CNV loss	22q11.21(20400132-21086225)x1	L1A;L2A;L3B;L4E;L5H	P-1.70	HP:0001249-Intellectual disability;HP:0000347-Micrognathia;HP:0030084-Clinodactyly
140901	F	Velocardiofacial syndrome	Chr.22q11.21del	GRCh[38]-CNV loss	22q11.21(20400132-21086225)x1	L1A;L2A;L3B;L4E;L5H	P-1.70	HP:0001249-Intellectual disability; HP:0007894-Hypopigmentation of the fundus ;Nystagmus-HP:0000639;HP:0001290-Generalized hypotonia;HP:0001388-Joint laxity;
R641	M	Velocardiofacial syndrome	Chr.22q11.21del	GRCh[38]-CNV loss	22q11.21(21444416-22574173)x1	L1A;L2A;L3C;L4C;L5F	P-2.00	HP:0001249-Intellectual disability;
141494	F	Velocardiofacial syndrome	Chr.22q11.21del	GRCh[38]-CNV loss	22q11.21(21444416-22574173)x1	L1A;L2A;L3C;L4B;L5A	P-2.50	HP:0001249-Intellectual disability; HP:0001627-Abnormal heart morphology;
S257	F	Velocardiofacial syndrome	Chr.22q11.21del	GRCh[38]-CNV loss	22q11.21(20721287-21025669)x1	L1A;L3A;L4C;L5A	VUS-0.55	HP:0001249-Intellectual disability; HP:0000104-Renal agenesis;HP:0007874-Almond-shaped palpebral fissure;HP:0001363-Craniosynostosis; HP:0010823-Ridged cranial sutures;HP:0002553-Highly arched eyebrow;HP:0001252-Hypotonia;HP:0000347-Micrognathia; HP:0011451-Primary microcephaly; HP:0002079-Hypoplasia of the corpus callosum;
131777	M	Velocardiofacial syndrome	Chr.22q11.21del	GRCh[38]-CNV loss	22q11.22(21968733-22215491)x1	L1A;L3A;L4E;L5F	VUS-0.10	HP:0007429-Few cafe-au-lait spots;HP:0009719-Hypomelanotic macule;HP:0000729-Autistic behavior
GM194370	M	Velocardiofacial syndrome	Chr.22q11.21del	GRCh[38]-CNV loss	22q11.22(21968733-22215491)x1	L1A;L2B;L3A;L4C;L5F	VUS-0.10	HP:0007272-Progressive psychomotor deterioration;
GM193223	M	Velocardiofacial syndrome	Chr.22q11.21del	GRCh[38]-CNV loss	22q11.22(21968733-22215491)x1	L1A;L3A;L4J;L5B	VUS(-0.60)	HP:0000717-Autism

GM191544	M	Velocardiofacial syndrome	Chr.22q11.21del	GRCh[38]-CNV loss	22q11.22(22655814-23285204)x1	L1A;L2B;L3C;L4J;L5E	VUS-0.30	HP:0002355-Difficulty walking;HP:0001263-Global developmental delay;
GM193550	M	Velocardiofacial syndrome	Chr.22q11.21del	GRCh[38]-CNV loss	22q11.22(22655814-23285204)x1	L1A;L2B;L3C;L4J;L5E	VUS-0.30	HP:0007018-Attention deficit hyperactivity disorder; HP:0001268-Mental deterioration
XCI cases screening (20)								
NWM-021D	F	Syndromic intellectual disability	/	/	/	/	/	HP:0001249-Intellectual disability; HP:0000717-Autism;HP:0001257-Spasticity; HP:0001347-Hyperreflexia;HP:0009487-Ulnar deviation of the hand;HP:0100702-Arachnoid cyst;HP:0002280-Enlarged cisterna magna;HP:0000383-Abnormality of periauricular region;HP:0000372-Abnormality of the auditory canal;HP:0000413-Atresia of the external auditory canal;HP:0000581-Blepharophimosis;HP:0000508-Ptoxis;HP:0005280-Depressed nasal bridge;HP:0000537-Epicanthus inversus
141078	M	XCI skewing	/	/				
162199	M	XCI skewing	/	/				
150692	M	XCI skewing	/	/				
140041	M	XCI skewing	/	/				
160035	M	XCI skewing	/	/				
152994	F	XCI skewing	/	/				
141345	F	XCI skewing	/	/				
210581	F	XCI skewing	/	/				
150689	F	XCI skewing	/	/				
170809	F	XCI skewing	/	/				
29D	F	XCI skewing	/	/				
6D	F	XCI skewing	/	/				
173D	F	XCI skewing	/	/				
164D	M	XCI skewing	/	/				
FM0711016_92	M	XCI skewing	/	/				
90D	M	XCI skewing	/	/				
43D	M	XCI skewing	/	/				
22D	M	XCI skewing	/	/				
111092	M	ATRX-like phenotype	ATRX	NM_000489.6	c.134-4884_242+41del	L1A;L2E;L3A;L5D	P-1.20	HP:0010864-Intellectual disability, severe, HP:0000286/Epicanthus , HP:0010806/U-Shaped upper lip vermilion, HP:0000194-Open mouth, HP:0001883-Talipes, HP:0002307-Drooling, HP:0001270-Motor delay , HP:0001344-Absent speech, HP:0012736-Profound global developmental delay

**Supplemental Table 2: filtered genome sequencing variants for cases 150163 and 218D (see link-
<https://www.medrxiv.org/content/10.1101/2022.09.18.22277970v1> (patient 4722))**

<i>NIPBL</i> (NM_133433.4)	effect	GnomAD	Inheritance
c.-80+35690G>A (intron 1/46)	no effect?	not reported	paternal
c.1495+3191A>G (intron 9/46)	New donor splice site: Activation of a cryptic donor site.	not reported	paternal
c.7861-1201G>C (intron 45/46)	Alteration of auxiliary sequence: Significant alteration if ESE/ESS motifs ration	not reported	paternal

Supplemental table 3: SMARCA2 tested variants

Variant	Category
NM_001289396.1(SMARCA2):c.1477_1479del, p.(Lys493del)	BAFopathy
NM_001289396.1(SMARCA2):c.2255G>C, p.(Gly752Ala)	BAFopathy
NM_001289396.1(SMARCA2):c.2261G>C, p.(Gly754Ala)	BAFopathy
NM_001289396.1(SMARCA2):c.2264A>G, p.(Lys755Arg)	BAFopathy
NM_001289396.1(SMARCA2):c.2348C>G, p.(Ser783Trp)	BAFopathy
NM_001289396.1(SMARCA2):c.2486C>T, p.(Thr829Ile)	BAFopathy
NM_001289396.1(SMARCA2):c.2558G>T, p.(Gly853Val)	BAFopathy
NM_001289396.1(SMARCA2):c.2564G>C, p.(Arg855Pro)	BAFopathy
NM_001289396.1(SMARCA2):c.2639C>T, p.(Thr880Ile)	BAFopathy
NM_001289396.1(SMARCA2):c.2642G>T, p.(Gly881Val)	BAFopathy
NM_001289396.1(SMARCA2):c.2647C>G, p.(Pro883Ala)	BAFopathy
NM_001289396.1(SMARCA2):c.2648C>T, p.(Pro883Leu)	BAFopathy
NM_001289396.1(SMARCA2):c.2671C>T, p.(Leu891Phe)	BAFopathy
NM_001289396.1(SMARCA2):c.2744C>A, p.(Ala915Asp)	BAFopathy
NM_001289396.1(SMARCA2):c.3209T>A, p.(Leu1070Gln)	BAFopathy
NM_001289396.1(SMARCA2):c.3313C>A, p.(Arg1105Ser)	BAFopathy
NM_001289396.1(SMARCA2):c.3404T>C, p.(Leu1135Pro)	BAFopathy
NM_001289396.1(SMARCA2):c.3464A>C, p.(Gln1155Pro)	BAFopathy
NM_001289396.1(SMARCA2):c.3475C>G, p.(Arg1159Gly)	BAFopathy
NM_001289396.1(SMARCA2):c.3476G>T, p.(Arg1159Leu)	BAFopathy
NM_001289396.1(SMARCA2):c.3485G>A, p.(Arg1162His)	BAFopathy
NM_001289396.1(SMARCA2):c.3493C>A, p.(Gln1165Lys)	BAFopathy
NM_001289396.1(SMARCA2):c.3573G>C, p.(Lys1191Asn)	BAFopathy
NM_001289396.1(SMARCA2):c.3602C>T, p.(Ala1201Val)	BAFopathy
NM_001289396.1(SMARCA2):c.3623C>G, p.(Ser1208Cys)	BAFopathy
NM_001289396.1(SMARCA2):c.3849G>T, p.(Trp1283Cys)	BAFopathy
NM_001289396.1(SMARCA2):c.1458C>G, p.(Asn486Lys)	BIS
NM_001289396.1(SMARCA2):c.1534G>A, p.(Glu512Lys)	BIS
NM_001289396.1(SMARCA2):c.1538G>T, p.(Gly513Val)	BIS
NM_001289396.1(SMARCA2):c.1573C>T, p.(Arg525Cys)	BIS
NM_001289396.1(SMARCA2):c.1574G>A, p.(Arg525His)	BIS
NM_001289396.1(SMARCA2):c.1585C>G, p.(Leu529Val)	BIS
NM_001289396.1(SMARCA2):c.2566A>G, p.(Met856Val)	BIS
NM_001289396.1(SMARCA2):c.2725T>A, p.(Phe909Ile)	BIS
NM_001289396.1(SMARCA2):c.2809C>T, p.(Arg937Cys)	BIS
NM_001289396.1(SMARCA2):c.2810G>A, p.(Arg937His)	BIS

Supplemental Materials and methods

X chromosome inactivation (XCI) analysis

XCI was tested in blood extracted DNA using an in-house developed protocol, as previously described.¹ In short, the XCI pattern was calculated using three microsatellite polymorphic markers to avoid uninformative results: (i) the CA-repeat in the promoter region of the SLIT and NTRK Like Family Member 4 (*SLITRK4*) gene; (ii) the CAG-repeat located in exon 1 of androgen receptor (*AR*) gene; (iii) the CA and AG tandem repeats in the first intron of Proprotein Convertase Subtilisin/Kexin Type 1 Inhibitor (*PCSK1N*) gene.

Genome sequencing analysis for case 150163

Genome sequencing was outsourced to BGI (Sequencing Platform: DNBseq; Sequencing read Length: PE100). After sequencing, raw data with adapter sequences or low-quality sequences were filtered using the SOAPnuke software (filter parameters: " -n 0.001 -l 10 --adaMR 0.25 --minReadLen 100"). We obtained 540,292,479 clean reads for a total of 108,058,495,800 bases. Q20: 98.56; Q30: 94.75.

Raw sequences were processed and analyzed using an in-house implemented pipeline previously described^{2,3} which is based on the GATK Best Practices.⁴ Briefly, in the pre-processing step reads were aligned to the GRCh38 genome assembly using BWA-MEM,⁵ duplicates were marked with samtools,⁶ markdup (v1.16) and base quality scores recalibrated with GATK⁴ (v4.2.1) BaseRecalibrator and ApplyBQSR. Single Nucleotide Variants (SNVs) and insertions and deletions <50 bp were called using GATK HaplotypeCaller and GenotypeGVCFs. We used Ensembl VEP v.104⁷ and dbNSFP v.4.0⁷ tools for variants functional annotation, including Combined Annotation Dependent Depletion (CADD) v.1.3,⁸ Mendelian Clinically Applicable Pathogenicity (M-CAP) v.1.0⁹ and Intervar v.0.1.6 for functional impact prediction.¹⁰

Thereby, the analysis was narrowed to variants which affect coding sequences or splice site regions. Moreover, high-quality variants were filtered against public databases (dbSNP150 and GnomAD ver.2.0.1) so that only variants with unknown frequency or having MAF <0.1%, as well as variants occurring with frequency < 1% in our population-matched database (~2000 exomes) were considered. Structural Variations (SVs) were called using Manta v1.6.0,⁸ Delly v1.1.6,⁹ SvABA v1.1.0,¹⁰ and LUMPY v0.3.1,¹¹ and individual results were combined in a single VCF file using a home-made script. The resulting VCF file was annotated using AnnotSV v3.1.3,¹² and subsequently filtered by removing SVs found in population databases with a frequency > 1% or in the ENCODE blacklist.

We carefully verified the presence of rare variants in the genomic region of the five known CdLS genes (*NIPBL*, *SMC1A*, *SMC3*, *RAD21*, *HDAC8*).

Supplemental References

1. Giovenino C, Trajkova S, Pavinato L, et al. Skewed X-chromosome inactivation in unsolved neurodevelopmental disease cases can guide re-evaluation For X-linked genes. *Eur J Hum Genet.* 2023.
2. Bauer CK, Calligari P, Radio FC, et al. Mutations in KCNK4 that Affect Gating Cause a Recognizable Neurodevelopmental Syndrome. *Am J Hum Genet.* 2018;103(4):621-630.
3. Flex E, Martinelli S, Van Dijck A, et al. Aberrant Function of the C-Terminal Tail of HIST1H1E Accelerates Cellular Senescence and Causes Premature Aging. *Am J Hum Genet.* 2019;105(3):493-508.
4. Van der Auwera GA, Carneiro MO, Hartl C, et al. From FastQ data to high confidence variant calls: the Genome Analysis Toolkit best practices pipeline. *Curr Protoc Bioinformatics.* 2013;43:11 10 11-33.
5. Li H, Durbin R. Fast and accurate long-read alignment with Burrows-Wheeler transform. *Bioinformatics.* 2010;26(5):589-595.
6. Danecek P, Bonfield JK, Liddle J, et al. Twelve years of SAMtools and BCFtools. *Gigascience.* 2021;10(2).
7. McLaren W, Gil L, Hunt SE, et al. The Ensembl Variant Effect Predictor. *Genome Biol.* 2016;17(1):122.
8. Chen X, Schulz-Trieglaff O, Shaw R, et al. Manta: rapid detection of structural variants and indels for germline and cancer sequencing applications. *Bioinformatics.* 2016;32(8):1220-1222.
9. Rausch T, Zichner T, Schlattl A, Stütz AM, Benes V, Korbel JO. DELLY: structural variant discovery by integrated paired-end and split-read analysis. *Bioinformatics.* 2012;28(18):i333-i339.
10. Wala JA, Bandopadhyay P, Greenwald NF, et al. SvABA: genome-wide detection of structural variants and indels by local assembly. *Genome Res.* 2018;28(4):581-591.
11. Layer RM, Chiang C, Quinlan AR, Hall IM. LUMPY: a probabilistic framework for structural variant discovery. *Genome Biol.* 2014;15(6):R84.
12. Geoffroy V, Herenger Y, Kress A, et al. AnnotSV: an integrated tool for structural variations annotation. *Bioinformatics.* 2018;34(20):3572-3574.
13. Gerber CB, Fliedner A, Bartsch O, et al. Further characterization of Borjeson-Forssman-Lehmann syndrome in females due to de novo variants in PHF6. *Clin Genet.* 2022;102(3):182-190.
14. Allen MD, Freund SM, Zinzalla G, Bycroft M. The SWI/SNF Subunit INI1 Contains an N-Terminal Winged Helix DNA Binding Domain that Is a Target for Mutations in Schwannomatosis. *Structure.* 2015;23(7):1344-1349.